CERN-TH/98-390
PITHA 98/41

Effects of Higgs sector CP violation in top-quark pair production at the LHC*

W. Bernreuther[a,b], A. Brandenburg[a] and M. Flesch[a]

[a] Institut f. Theoretische Physik, RWTH Aachen, D-52056 Aachen, Germany
[b] Theory Division, CERN, CH-1211 Geneva 23, Switzerland

Abstract:
A striking manifestation of CP violation in the electroweak symmetry breaking sector would be the existence of neutral Higgs boson(s) with undefined CP parity. We analyse signatures of such a boson, with a mass of about 300 GeV or larger, produced in high energy proton-proton collisions at LHC energies in its top-quark antitop-quark decay channel. The large irreducible $t\bar{t}$ background is taken into account. We propose, both for the dilepton and the lepton + jets decay channels of $t\bar{t}$, several correlations and asymmetries with which (Higgs sector) CP violation can be traced. We show that for judiciously chosen cuts on the $t\bar{t}$ invariant mass these CP observables yield, for an LHC integrated luminosity of 100 fb^{-1}, statistically significant signals for a range of Higgs boson masses and Yukawa couplings.

PACS number(s): 11.30.Er, 12.60.Fr, 14.65.Ha, 14.80.Cp
Keywords: hadron collider physics, top quarks, Higgs bosons, CP violation

*Work supported by D.F.G. and by BMBF contract 05 7AC 9EP.

1 Introduction

The clarification of the mechanism of electroweak gauge-symmetry breaking will be among the most important physics issues at the CERN Large Hadron Collider (LHC). According to the concept used in the Standard Model (SM) and in many of its extensions, this amounts to searching for Higgs bosons. While in the standard electroweak theory (SM) only one neutral Higgs boson is associated with electroweak symmetry breaking, many extensions of the SM entail a more complex scalar sector. Apart from predicting a number of Higgs particles, an extended scalar sector can also have a bearing on another phenomenon of unclarified origin, namely CP non-conservation. As is well-known CP can be violated by an extended Higgs sector [1]. As far as the neutral Higgs bosons are concerned, this would manifest itself in neutral spin-zero states of undefined CP parity, i.e. particles that have both scalar and pseudoscalar Yukawa couplings to quarks and leptons [2]. This possibility arises naturally already in two-Higgs doublet extensions of the SM [1, 3, 4, 5]. As to supersymmetric extensions of the SM, mixing of the CP $= +1$ and CP $= -1$ neutral Higgs-boson states, leading to CP-impure mass eigenstates, can also occur at tree level in its next-to-minimal extension (NMSSM) [6], while in the minimal extension (MSSM) mixing is induced radiatively and can be quite substantial [7, 8], depending on the parameters of the model.

If Higgs boson(s) will be discovered, the most direct way to study their CP properties at the LHC will be the investigation of their Yukawa interactions with top quarks. For a neutral Higgs boson φ of arbitrary CP parity and mass $m_\varphi > 2m_t$, CP violation occurs already at the Born level in its decay[1] $\varphi \to t\bar{t}$ and shows up in spin-spin correlations [9] – [12]. However, the effect is diluted by interference with the $t\bar{t}$ background [9, 10]. Effects of CP-violating φ boson exchange in $pp \to t\bar{t}X$ were analysed in [14, 9, 10, 15]. Concerning the study of Yukawa couplings of a light neutral Higgs boson φ with a mass of about 100 GeV at the LHC, associated $t\bar{t}\varphi$ production [16] and the decay mode $\varphi \to \tau^+\tau^-$ [9, 12] offer further possibilities. CP effects in $t\bar{t}$ production and decay at hadron colliders were also investigated in terms of form factor parametrizations [17] – [21], within the MSSM [22, 15], and for single top-quark production within two-Higgs doublet models and the MSSM [23, 24].

In this article we investigate the signatures of a heavy Higgs boson of arbitrary CP parity in the $pp \to t\bar{t}X$ channel at the LHC, taking the irreducible $t\bar{t}$ background into account. We extend previous analyses and obtain several new results. We propose, for the dilepton and the lepton + jets decay channels of $t\bar{t}$, a number of CP observables and associated asymmetries that should be rather robust with respect to measurement uncertainties. We analyse, within two-Higgs doublet and supersymmetric extensions of the SM, the sensitivity of these observables to CP-violating contributions from the $t\bar{t}$ production and top-quark decay amplitudes. By using appropriate bins in the $t\bar{t}$ invariant-mass distribution we show that, for a range of Higgs boson masses and Yukawa couplings, these observables and asymmetries exhibit CP effects at the percent level. Thus these

[1] For the channels $\varphi \to W^+W^-, ZZ$ CP violation can take place only at the one-loop level (see, e.g., [11, 13]) and is therefore expected to lead to smaller effects.

quantities should be good tools for tracing Higgs sector CP violation in future LHC experiments.

Our paper is organized as follows. In section 2 we recapitulate the salient features of neutral Higgs sector CP violation within two-Higgs doublet and supersymmetric extensions of the SM, which are relevant to our analysis, and we outline the strategy of how to trace possible CP effects caused by a heavy Higgs boson s-channel resonance in $pp \to t\bar{t}X$. In section 3 we discuss the general structure of the squared matrix elements for the parton reactions $gg, q\bar{q} \to t\bar{t} \to W^+bW^-\bar{b} \to 6f$ in the on-shell approximation for t and $\bar{t}$ quarks using the spin-density matrix formalism. We exhibit the two types of CP-odd spin-momentum correlations which are induced at the level of the $t\bar{t}$ states and argue that CP violation effects in $t \to Wb$ are small compared with (quasi)resonant φ exchange in $t\bar{t}$ production. In section 4 we introduce a number of CP observables and asymmetries with which CP violation effects can be traced in $pp \to t\bar{t}X$ in the dilepton and the lepton + jets channels, and we derive relations between expectation values of observables and corresponding asymmetries. We show that those of our observables that are T-odd are predominantly sensitive to CP-violating terms in the $t\bar{t}$ production amplitude, irrespective of whether φ is heavy or light. In section 5 we compute and plot, for the c.m. energy $\sqrt{s} = 14$ TeV and for a set of Higgs boson masses and Yukawa couplings, the expectation values of two CP observables as a function of the $t\bar{t}$ invariant mass $M_{t\bar{t}}$, taking resonant and non-resonant Higgs boson exchange and the irreducible $t\bar{t}$ background into account. These plots serve to select appropriate $M_{t\bar{t}}$ bins in the computation of the expectation values and asymmetries of the CP observables of section 4. These calculations are then performed for the dilepton and lepton + jets channels, using phase-space cuts on the transverse momenta of the final state leptons and partons. Finally we estimate, for an LHC integrated luminosity of 100 fb^{-1}, the statistical sensitivity of these observables to Higgs sector CP violation, i.e. the sensitivity of these observables to detect a non-zero product of scalar and pseudoscalar Yukawa couplings. We conclude in section 6. In the appendix we give a compact formula for computing the expectation values of the CP observables.

2 Higgs sector CP violation

A number of extensions of the Standard Model allow for the possibility of CP violation in the Higgs sector, the simplest ones being extensions by an additional Higgs doublet [1, 3, 4, 5]. For definiteness we consider two-Higgs doublet extensions with natural flavour conservation at the tree level and explicit CP violation, both by complex Yukawa coupling matrices, which lead to a Kobayashi-Maskawa (KM) phase [25], and by the tree-level Higgs potential $V(\Phi_1, \Phi_2)$ (see, e.g., [5]). As a consequence of the latter the three physical neutral scalar mass eigenstates $\varphi_{1,2,3}$ of these models are not CP eigenstates, i.e. they couple to both scalar and pseudoscalar quark and lepton currents. Using the same symbols for the corresponding scalar fields we have

$$\mathcal{L}_Y = -(\sqrt{2}G_F)^{1/2} \sum_{j,f} m_f (a_{jf}\bar{f}f + \tilde{a}_{jf}\bar{f}i\gamma_5 f)\,\varphi_j \ , \tag{1}$$

where G_F is Fermi's constant, f denotes a quark or lepton field and m_f its associated mass, and $a_{jf}, \tilde{a}_{jf}$ are the reduced scalar and pseudoscalar Yukawa couplings, respectively, which depend on the parameters of the scalar potential and on the type of model. For example, in the model where the Higgs doublet $\Phi_2(\Phi_1)$ gives mass to the $u(d)$-type quarks (called model II in the literature) these couplings read [26]

$$\begin{aligned} a_{ju} &= d_{2j}/\sin\beta \ , \quad \tilde{a}_{ju} = -d_{3j}\cot\beta \ , \\ a_{jd} &= d_{1j}/\cos\beta \ , \quad \tilde{a}_{jd} = -d_{3j}\tan\beta \ , \end{aligned} \tag{2}$$

where u, d labels the charge $2/3$ and $-1/3$ quarks, respectively, $\tan\beta = v_2/v_1$ is the ratio of (the moduli of) vacuum expectation values of the two Higgs doublets, and (d_{ij}) is a 3×3 orthogonal matrix that describes the mixing of the neutral scalar states. In the model where one Higgs doublet gives mass to both the u- and d-type quarks (called model I) one has $a_{jd} = a_{ju}$ and $\tilde{a}_{jd} = \tilde{a}_{ju}$. If this doublet is Φ_2 then $a_{ju}, \tilde{a}_{ju}$ are the same as in (2). (In the SM $a = 1$, $\tilde{a} = 0$.) At the Born level only the CP $= +1$ component of φ couples to W^+W^- and to ZZ. The couplings are given by the respective SM couplings times the factor $g_{VV} = (d_{11}\cos\beta + d_{21}\sin\beta), V = W, Z$.

In addition, the particle spectrum contains a charged Higgs boson $H^\pm$. In models with natural flavour conservation at tree level, $H^\pm$ exchange transports the KM phase and does not lead to significant CP effects of the type discussed below. Experimental data on $b \to s + \gamma$ yield, for type II models, a lower bound on the mass of $H^\pm$, which is $m_{H^+} > 200$ GeV for $\tan\beta \leq 1$ [27].

The effects analysed below are significant only if the reduced Yukawa couplings of φ to the t quark are not very much suppressed as compared with those of the SM – if suppressed at all. Within two-Higgs doublet extensions one should have $\tan\beta$ of order 1 or smaller. On the other hand the measured strength of neutral K and B meson mixing provides a lower bound on $\tan\beta$. From studies of the meson mixing amplitudes in these models [28] one infers that $\tan\beta \gtrsim 0.3$. An important constraint on non-standard (Higgs sector) CP violation is provided by the experimental upper bounds of the electric dipole moments (EDMs) of the neutron [29] and of the electron [30]. A reanalysis of these moments within two-Higgs doublet models was made in [31], assuming so-called maximal CP violation in the neutral Higgs sector, which in our parametrization may be defined by putting $|d_{11}| = |d_{21}| = |d_{31}| = 1/\sqrt{3}$. From this study one deduces that $|a_{jt}\tilde{a}_{jt}| \lesssim 2$ is compatible with these low-energy constraints. It should be noted that this bound is subject to considerable theoretical uncertainties in the estimates of hadronic matrix elements that are needed in the computation of the neutron EDM [32, 33].

In the next-to-minimal supersymmetric extension of the SM with two $SU(2)$ Higgs doublets $\Phi_{1,2}$ and one gauge singlet N, the Higgs potential $V(\Phi_1, \Phi_2, N)$ can be CP-violating at tree level, leading again to neutral scalar mass eigenstates with undefined CP parity [6]. As far as the minimal supersymmetric extension of the SM with soft supersymmetry breaking terms is concerned, it is well-known that the tree-level Higgs potential $V(\Phi_1, \Phi_2)$ is CP-invariant. Nevertheless, CP-violating phases in the soft SUSY-breaking terms can induce mixing of the CP $= +1$ neutral scalar Higgs boson states h, H with the CP $= -1$ state A at the one-loop level. It was recently pointed out [8] that in a

large region of the parameter space of the MSSM, where the heavy states H and A are almost mass-degenerate at tree level, sizeable radiative mixing of H and A can be induced by CP-violating Yukawa couplings involving scalar quarks of the third generation.

In the following we study, in a quite model-independent fashion, the effects on $t\bar{t}$ production at the LHC of a heavy Higgs boson resonance φ with mass $m_\varphi > 300$ GeV, which is not a CP eigenstate. For definiteness we choose in section 5 a range of reduced scalar and pseudoscalar Yukawa couplings to t quarks, denoted by $a, \tilde{a}$ in the following, between $0.3 \leq |a|, |\tilde{a}| \leq 1$, and a reduced coupling $|g_{VV}| \leq 0.4$ to W^+W^- and ZZ. A straightforward exercise yields that the chosen range of couplings is compatible with the empirical bound $\tan\beta \gtrsim 0.3$. Larger values of $|a\tilde{a}|$ would, of course, increase the effects computed in section 5. Our choice of values for g_{VV} is somewhat arbitrary. However, because the CP effects below decrease for $|g_{VV}| \to 1$, we are interested in φ-boson couplings to W^+W^- and ZZ bosons that are smaller than the corresponding SM couplings. For instance this is the case for φ states with a substantial pseudoscalar component.

If $m_\varphi > 2m_t$, the total φ decay width is then given, to good approximation, by the sum of the widths of φ decay into $t\bar{t}$, W^+W^-, and ZZ, which we compute in terms of $a, \tilde{a}$, and g_{VV} (see Eq. (48)). The parameter

$$\gamma_{CP} \equiv -a\tilde{a} \tag{3}$$

serves as a measure of Higgs sector CP violation.

Finally a few words on why it is justified to take into account below the exchange of only one φ_j boson. One should recall that a necessary condition of observable CP violation in the neutral Higgs sector is a non-degenerate mass spectrum of the neutral states. Even if the products of couplings $a_{jt}\tilde{a}_{jt}$ are of the same order of magnitude the CP effects caused by φ_j bosons with mass markedly below $2m_t$ are significantly smaller [14, 10] than the effects due to heavier bosons which appear as resonances in $gg \to t\bar{t}$. If one evaluates CP observables $\mathcal{O}$ on the whole $t\bar{t}$ sample, all φ_j exchanges must be taken into account. Even if some or all of the products $|a_{jt}\tilde{a}_{jt}|$ are of order 1, considerable cancellations among the contributions to $\langle\, \mathcal{O}\, \rangle$ may nevertheless occur. This is because of the orthogonality of the mixing matrix (d_{ij}), $\sum_j d_{1j}d_{3j} = 0$. However, what we have in mind are CP studies *after* one heavy Higgs boson (or several) would have been discovered, and seen as a resonance in the invariant $t\bar{t}$ mass distribution $d\sigma/dM_{t\bar{t}}$. It was shown in [34] that there is a statistically significant signal in this spectrum for the above range of couplings. Then the CP observables proposed in section 4 are to be measured on data samples which will be selected by appropriately chosen cuts on $M_{t\bar{t}}$ in the vicinity of m_φ. In this way the CP properties of this boson can be investigated experimentally.

3 Matrix elements

Next we investigate $t\bar{t}$ production in high-energy pp collisions by the main parton reactions $gg, q\bar{q} \to t\bar{t} \to 6f$. At the level of these reactions the exchange of a Higgs boson φ with couplings (1) induces CP-odd t and $\bar{t}$ spin-momentum correlations, which, through t and

$\bar{t}$ decay, lead to characteristic angular correlations and asymmetries among the decay products of these quarks.

At high energy hadron colliders, such as the LHC, a φ boson with mass not more than about 600 GeV will be produced dominantly by gluon-gluon fusion through a virtual top-quark loop. This holds true also for the multi-Higgs doublet extensions of the SM in the parameter space of interest to us, namely $\tan\beta$ of order 1. Then $gg \to \varphi$ production through b-quark loops can be safely neglected. Likewise, when considering (N)MSSM models, squark loops can be neglected in this production mechanism if squark masses are larger than 400 GeV [35], which we shall assume. The next-to-leading QCD corrections for scalar and pseudoscalar Higgs-boson production were computed in [36] – [38] and were found to increase the cross section significantly. (For the SM electroweak corrections to $t\bar{t}$ production, including s-channel Higgs boson exchange, see [39].) Here we study the signal and the background amplitudes only to lowest order in the QCD coupling. (Computing the QCD corrections to these amplitudes for *polarized* t and $\bar{t}$ quarks is a task beyond the scope of this paper.) This can be justified as we do not investigate cross sections but normalized distributions. More specifically, non-zero expectation values of the observables which we study in sections 4 and 5 cannot be generated by QCD corrections – but by $\gamma_{CP} \neq 0$.

The $\varphi \to t\bar{t}$ decay channel is affected by the large non-resonant $t\bar{t}$ background. The amplitudes $gg \to \varphi \to t\bar{t}$ and $gg \to t\bar{t}$ interfere and produce at the parton level a characteristic peak-dip structure in a number of observables [40, 9, 10, 41, 34] if the $t\bar{t}$ invariant mass lies in the vicinity of the Higgs boson mass. In [34] it was found that a heavy φ boson of arbitrary CP nature yields – for a range of reduced Yukawa and vector boson couplings $a, \tilde{a}$ and g_{VV} – a statistically significant signal in the $t\bar{t}$ invariant mass distribution. Here we are interested in φ-induced t and $\bar{t}$ spin polarization and spin-correlation effects which reveal the nature of the Yukawa couplings of φ. For this purpose we consider the $t\bar{t}$ production density matrices for the parton processes $\lambda\bar{\lambda} \to t\bar{t}$ ($\lambda = q, g$). They are defined by

$$R^{(\lambda)}_{\alpha\alpha',\beta\beta'} = \frac{1}{n_{(\lambda)}} \sum_{\substack{\text{colours} \\ \text{initial spins}}} \langle t_\alpha \bar{t}_\beta | \mathcal{T} | \, \lambda\bar{\lambda} \, \rangle \, \langle \, \lambda\bar{\lambda} \, | \mathcal{T}^\dagger | t_{\alpha'} \bar{t}_{\beta'} \rangle \; , \tag{4}$$

where the factor $n_{(\lambda)}$ averages over spin and colour of the initial state partons; $n_{(q)} = (2N_C)^2 = 36$, $n_{(g)} = (2(N_C^2 - 1))^2 = 256$. The matrices $R^{(\lambda)}$ are of the form

$$\begin{aligned} R^{(\lambda)}_{\alpha\alpha',\beta\beta'} \;\; = \;\; & A^{(\lambda)} \delta_{\alpha\alpha'} \delta_{\beta\beta'} + B^{(\lambda)}_{+i} \hat{k}_i (\sigma^i)_{\alpha\alpha'} \delta_{\beta\beta'} + B^{(\lambda)}_{-i} \delta_{\alpha\alpha'} (\sigma^i)_{\beta\beta'} \\ & + C^{(\lambda)}_{ij} (\sigma^i)_{\alpha\alpha'} (\sigma^j)_{\beta\beta'} \; , \end{aligned} \tag{5}$$

where σ^i are the Pauli matrices. Using rotational invariance the vectors $B^{(\lambda)}_{\pm i}$ and tensors $C^{(\lambda)}_{ij}$ can be further decomposed. A general discussion of the symmetry properties of these matrices and their decomposition in the t and $\bar{t}$ spin spaces is given in [9, 10].

As we are concerned with CP-violating Higgs-boson effects, we take into account the QCD Born amplitudes for $q\bar{q}, gg \to t\bar{t}$ and all φ exchange terms proportional to $\alpha_s \gamma_{CP}$,

that is, the CP-violating pieces of the one-loop self-energy, vertex, and box diagram contributions. If $m_\varphi > 2m_t$ the s-channel φ-exchange diagram $gg \to \varphi \to t\bar{t}$ is by far the most important φ contribution. The spin density matrices $R^{(\lambda)}$ were computed in [9, 10] and these calculations were recently confirmed in [15].

Heavy φ exchange leaves, for γ_{CP} of order 1, also a markedly larger signal in our CP observables (given below and in the next section) than CP-violating gluino exchange in $q\bar{q}, gg \to t\bar{t}$, which was computed in [22, 15]. Therefore we omit such effects below.

At the level of the $t\bar{t}$ states the CP-violating interaction (1) generates two types of CP-odd spin-momentum correlation terms in (5), namely

$$\hat{\mathbf{k}}_t \cdot (\mathbf{s}_t - \mathbf{s}_{\bar{t}}) f_e(z) \ , \tag{6}$$

$$\hat{\mathbf{p}} \cdot (\mathbf{s}_t - \mathbf{s}_{\bar{t}}) f_o(z) \ , \tag{7}$$

and

$$\hat{\mathbf{k}}_t \cdot (\mathbf{s}_t \times \mathbf{s}_{\bar{t}}) h_e(z) \ , \tag{8}$$

$$\hat{\mathbf{p}} \cdot (\mathbf{s}_t \times \mathbf{s}_{\bar{t}}) h_o(z) \ . \tag{9}$$

Here $\mathbf{s}_t, \mathbf{s}_{\bar{t}}$ are the spin operators of t and $\bar{t}$, and $\hat{\mathbf{k}}_t$ and $\hat{\mathbf{p}}$ are the unit vectors of the momenta of the top quark and of the initial parton λ, respectively, defined in the parton c.m. system. Here $\lambda = g, q, \bar{q}$ is the parton in the proton that moves by definition along the $+z$-direction. (Neglecting transverse parton momenta implies that $\hat{\mathbf{p}}$ is equal to the direction of the proton beam in the laboratory frame.) The functions f_e, h_e and f_o, h_o denote even and odd functions of the scattering angle $z = \cos\theta = \hat{\mathbf{p}} \cdot \hat{\mathbf{k}}_t$. The expressions (6) – (9) constitute a complete set of CP observables in the case at hand. Here the expectation value of an observable $\mathcal{O}$ for the respective parton reaction is defined as $\langle\, \mathcal{O}\, \rangle_\lambda = \int_{-1}^{1} dz \mathrm{Tr}(R^{(\lambda)}\mathcal{O})/N_\lambda$, where N_λ is a normalization factor. The observables (6), (7) are CP-odd but T-even, i.e. do not change sign under a naive T transformation (reversal of momenta and spins, but no interchange of initial and final states), whereas (8), (9) are CP-odd and T-odd. This implies that non-zero expectation values of (6), (7) require $\gamma_{CP} \neq 0$ and a non-zero absorptive part of the respective scattering amplitude, whereas (8), (9) are "dispersive" CP observables. (The CP asymmetry $\Delta N_{LR} = [N(t_L\bar{t}_L) - N(t_R\bar{t}_R)]/(\mathrm{all}\, t\bar{t})$ considered in [14] corresponds to the basic longitudinal polarization asymmetry $\langle\, \hat{\mathbf{k}}_t \cdot (\mathbf{s}_{\bar{t}} - \mathbf{s}_t)\, \rangle$.)

Furthermore it is worth pointing out the following. One might naively think that the CP-odd and T-odd observable

$$\mathcal{P}_{CP} \ = \ \hat{\mathbf{n}} \cdot (\mathbf{s}_t - \mathbf{s}_{\bar{t}})\, w(z) \ , \tag{10}$$

where $\hat{\mathbf{n}}$ is the unit vector corresponding to $\mathbf{n} = \mathbf{p} \times \mathbf{k}_t$ and w is some function of z, would also be of relevance here. (For $gg \to t\bar{t}$ Bose symmetry requires $w(z)$ to be an odd function.) It amounts to searching for a difference in the normal components of the t and $\bar{t}$ spin-polarizations. However, $\langle\, \mathcal{P}_{CP}\, \rangle_\lambda \neq 0$ requires C- and CP-violating interactions – but QCD and the Yukawa interaction (1) are C-invariant and thus do not generate terms of the form (10) in the above density matrices. The quantity $\mathcal{P}_{CP}$ and the corresponding

observables involving the charged lepton momenta from semileptonic t or $\bar{t}$ decay instead of the spin vectors $\mathbf{s}_t$ and $\mathbf{s}_{\bar{t}}$ (see section 4 for the analogous transcriptions of (6) and (8)) may nevertheless be used experimentally to check for C- and CP-violating interactions in $t\bar{t}$ production. Exchange of W and/or Z bosons in conjunction with φ exchange leads to such effects, but they are very small. (We note in passing that for $e^+e^- \to (\gamma^*, Z^*) \to t\bar{t}$ the difference of the normal polarizations of t and $\bar{t}$ is a relevant CP observable for tracing Higgs-sector CP violation [42].) On the other hand, absorptive parts due to QCD in the scattering amplitudes of the above parton reactions generate equal normal polarizations of t and $\bar{t}$, i.e. lead to T-odd terms of the form

$$\hat{\mathbf{n}} \cdot (\mathbf{s}_t + \mathbf{s}_{\bar{t}})\, w(z) \tag{11}$$

in the respective density matrices. The QCD-induced normal polarizations were computed in [43, 44]. It is also worth recalling the observation [9] that interactions being P- and CP-invariant cannot induce T-odd spin-spin correlations.

We have found that, for LHC energies, the spin-polarisation and spin-correlation observables (6),(8) which involve the helicity axis $\hat{\mathbf{k}}_t$ are more sensitive to a non-zero product γ_{CP} of reduced Yukawa couplings than the corresponding observables (7),(9) which involve the beam axis $\hat{\mathbf{p}}$. Therefore we shall consider only the former set of observables below. Moreover it was shown in [12, 34] that the CP-even spin-spin correlation observable $\mathbf{s}_t \cdot \mathbf{s}_{\bar{t}}$ is also sensitive to the Yukawa couplings $a, \tilde{a}$ and should therefore also be taken into account in these kind of investigations.

The t and $\bar{t}$ quarks auto-analyse their spins by their parity-violating weak decays. We shall assume that $t \to Wb$ is the dominant decay mode, as predicted by the SM. It is well-known that in the SM the most efficient analyser of the t spin is the charged lepton from subsequent W decay. Its spin analyser quality is more than twice as high as the W or b quark direction of flight.

We use the narrow width approximation for $t\bar{t}$ production and decay, which is justified because of Γ_t/m_t, $\Gamma_W/m_W \ll 1$ and because we are concerned only with normalized distributions and expectation values of observables. Moreover we take the leptons and the light quarks, including the b quark, to be massless. If the charged lepton from semileptonic t decay, $t \to \ell^+\nu_\ell b$, acts as t-spin analyser then, integrating out the b, ν_ℓ momenta, the t decay density matrix $\rho_{\alpha'\alpha}$ in the t rest frame is of the form $\rho_{\alpha'\alpha} = f(E_\ell)(\mathbb{1} + \boldsymbol{\sigma} \cdot \hat{\mathbf{q}}_+)_{\alpha'\alpha}$, where α', α are t spin indices, $\hat{\mathbf{q}}_+$ is the ℓ^+ direction of flight, and f is a function of the lepton energy E_ℓ (see, e.g., [45, 46]). This expression, which holds to lowest order in the SM, is respected by QCD corrections to a high degree of accuracy [47]. (The t, respectively $\bar{t}$ rest frame is defined by performing a rotation-free Lorentz boost from the parton c.m. system. The parton c.m. frame can be obtained from the laboratory frame by a rotation-free boost along the beam axis that depends on the momentum fractions $x_{1,2}$ of the partons. The t and $\bar{t}$ rest frames defined in this way differ by a Wigner rotation from the respective rest frames obtained by a direct rotation-free boost from the laboratory frame.)

One may also choose the b quark – or the W boson – to be the spin-analyser of the t

quark. This is an obvious choice for non-leptonic t decay and we shall employ it below[2]. In this case the t decay density matrix is given in the t rest frame by $\rho_{\alpha'\alpha} = (1\!\!1 - \kappa\,\boldsymbol{\sigma}\cdot\hat{\mathbf{q}}_b)_{\alpha'\alpha}$, where the t spin-analyser quality factor $\kappa = (1-2\mu)/(1+2\mu)$ with $\mu = m_W^2/m_t^2$. If the reconstructed W direction of flight is used instead of $\hat{\mathbf{q}}_b$, the corresponding t decay density matrix is obtained from this expression by substituting $\hat{\mathbf{q}}_b \to -\hat{\mathbf{q}}_{W^+}$. Numerically, $\kappa \approx 0.41$, which shows that in these cases the t spin analysing power is lower by more than a factor of two as compared to the charged lepton. The density matrices for $\bar{t}$ decay are obtained by substituting $\hat{\mathbf{q}}_+ \to -\hat{\mathbf{q}}_-, \hat{\mathbf{q}}_b \to -\hat{\mathbf{q}}_{\bar{b}}, \hat{\mathbf{q}}_{W^+} \to -\hat{\mathbf{q}}_{W^-}$ in the above expressions.

Suffice it to mention that SM CP violation in $t \to Wb$ is tiny [46], as in $t\bar{t}$ production. There is no effect to one-loop approximation in the amplitudes $q\bar{q}, gg \to t\bar{t}$. What about CP effects in $t \to Wb$ within the models discussed in the previous section? Although neutral φ exchange induces a CP-violating form factor[3] in the $t \to Wb$ vertex at the one-loop order, the resulting CP effect in top-quark decay is only a few per mille [48] and thus markedly smaller than the effects in $t\bar{t}$ production (see section 5). Within the (N)MSSM the form factors that are induced by CP-violating gluino [42], neutralino, and chargino exchanges [24] also lead to CP effects at the per mille level only. We shall omit these effects below. (A more specific discussion is given in section 4.)

Besides $t \to Wb$ also other decay modes/mechanisms may be relevant to top quark decay; for instance $t \to H^+b$, respectively $t \to b\tau\nu_\tau, bq\bar{q}'$ mediated by virtual H^+ exchange. In non-supersymmetric n-Higgs doublet models ($n \geq 2$) of type II, the lower bound on the mass of H^+ quoted above implies that in these models the H^+ mediated part of the decay amplitude $\mathcal{T}(t \to f)$ will be small with respect to the dominant part from (on-shell) W^+ exchange. (Here $f = b\ell\nu_\ell, bq\bar{q}'$.) However, charged Higgs bosons in type I or in SUSY models are not restricted by these data [27, 49]. Also a direct search made by the CDF collaboration at the Tevatron [50] does not yet severely constrain the decay mode $t \to H^+b$.

In any case, our analysis below is set up in a modular way and can always be straightforwardly extended if significant top decay modes and/or decay mechanisms other than $t \to Wb$ should be discovered. Moreover, in the next section we define observables that are mainly sensitive to CP violation in the $t\bar{t}$ production amplitude.

In summary, the squared matrix elements of the reactions $\lambda\bar{\lambda} \to t\bar{t} \to f_1 f_2$, which we use below, are of the form

$$\mathrm{Tr}\,[\rho^{(f_1)} R^{(\lambda)} \rho^{(f_2)}] \equiv \rho^{(f_1)}_{\alpha'\alpha} R^{(\lambda)}_{\alpha\alpha',\beta\beta'} \rho^{(f_2)}_{\beta'\beta}\ , \tag{12}$$

with production and decay density matrices as discussed above. At least as far as Higgs bosons with mass $m_\varphi \gtrsim 300$ GeV and reduced Yukawa couplings $a, \tilde{a}$ of order 1 in simple two-Higgs doublet models and the (N)MSSM are concerned, the most significant CP-violating contribution to this expression comes from (quasi-) resonant φ s-channel exchange and resides in $R^{(g)}$.

[2]In principle one could do better by identifying the u or d-type quark from $W \to q\bar{q}'$ decay either by tagging methods or from decay distribution characteristics.

[3]For a discussion of the symmetry properties of the form factors that can appear in this decay mode, see [45, 46].

4 Observables

In the following we consider two types of $t\bar{t}$ decay channels: first the "dilepton + jets" channels, where both t and $\bar{t}$ decay semileptonically,

$$t + \bar{t} \to W^+ b + W^- \bar{b} \to \ell^+ \nu_\ell b + \ell'^- \bar{\nu}_{\ell'} \bar{b} \; . \tag{13}$$

As mentioned above, the directions of flight of the charged leptons are the best analysers of the $t, \bar{t}$ spins.

Secondly we study the "lepton + jets" channels, where the t quark decays semileptonically and the $\bar{t}$ quark non-leptonically and vice versa. These channels also have a good signature for top-quark identification and they are suitable for determining the $t\bar{t}$ invariant-mass spectrum. Events where the top quark decays semileptonically and the top antiquark decays hadronically will be called sample $\mathcal{A}$:

$$\mathcal{A} : \left\{ \begin{array}{l} t \to W^+ b \to \ell^+ \nu_\ell b \; , \\ \bar{t} \to W^- \bar{b} \to q \bar{q}' \bar{b} \; , \end{array} \right. \tag{14}$$

while $\bar{\mathcal{A}}$ will denote the sample that consists of the charge-conjugated decay channels of the $t\bar{t}$ pairs:

$$\bar{\mathcal{A}} : \left\{ \begin{array}{l} t \to W^+ b \to \bar{q} q' b \, , \\ \bar{t} \to W^- \bar{b} \to \ell^- \bar{\nu}_\ell \bar{b} \; . \end{array} \right. \tag{15}$$

In (13) – (15) we take into account only semileptonic top decays into either an electron or a muon. Then the SM predicts, to a good approximation, a fraction of 24/81 of all $t\bar{t}$ events to decay into the single lepton channels and 4/81 into the dilepton channels.

For the dilepton channel the cross section measure reads in the narrow width approximation (12):

$$\begin{aligned} &\int d\sigma(pp \to t\bar{t}X \to \ell^+ \nu_\ell b + \ell'^- \bar{\nu}_{\ell'} \bar{b} + X) = \\ &\quad \mathcal{N} \sum_{\lambda = q, \bar{q}, g} \int_0^1 dx_1 \int_0^1 dx_2 \; N_\lambda(x_1) N_{\bar{\lambda}}(x_2) \Theta(\hat{s} - 4m_t^2) \\ &\quad \times \frac{\beta}{(4\pi)^2 \hat{s}} \int d\Omega_{\hat{\mathbf{k}}_t} \, \frac{1}{\eta} \int_\mu^1 dy_+ y_+ (1 - y_+) \frac{1}{\eta} \int_\mu^1 dy_- y_- (1 - y_-) \\ &\quad \times \int \frac{d\Omega_{\hat{\mathbf{q}}_+}}{4\pi} \int \frac{d\Omega_{\hat{\mathbf{q}}_-}}{4\pi} \left\{ A^{(\lambda)} + B^{(\lambda)}_{+i} \hat{q}_{+i} - B^{(\lambda)}_{-i} \hat{q}_{-i} - C^{(\lambda)}_{ij} \hat{q}_{+i} \hat{q}_{-j} \right\} \\ &\quad \times \int_0^\infty dE_b \, \delta \left(E_b - \frac{m_t^2 - m_W^2}{2m_t} \right) \int \frac{d\Omega_{\hat{\mathbf{q}}_b}}{2\pi} \, \delta \left(\hat{\mathbf{q}}_+ \cdot \hat{\mathbf{q}}_b - \frac{2\mu - y_+(1+\mu)}{y_+(1-\mu)} \right) \\ &\quad \times \int_0^\infty dE_{\bar{b}} \, \delta \left(E_{\bar{b}} - \frac{m_t^2 - m_W^2}{2m_t} \right) \int \frac{d\Omega_{\hat{\mathbf{q}}_{\bar{b}}}}{2\pi} \, \delta \left(\hat{\mathbf{q}}_- \cdot \hat{\mathbf{q}}_{\bar{b}} - \frac{2\mu - y_-(1+\mu)}{y_-(1-\mu)} \right) \; . \end{aligned} \tag{16}$$

In the first line on the r.h.s. $\mathcal{N} = BR(t \to b\ell^+\nu_\ell) BR(\bar{t} \to \bar{b}\ell^-\bar{\nu}_\ell)$ is the product of the semileptonic t and $\bar{t}$ branching ratios, and $N_\lambda(x_1)$, $N_{\bar{\lambda}}(x_2)$ are the parton distribution

functions. The next two lines in Eq. (16) represent (up to the factor $\mathcal{N}$) the cross section $\int d\hat{\sigma}^{(\lambda)}$ for the partonic subprocesses $\lambda\bar{\lambda} \to t\bar{t} \to \ell^+\nu_\ell b\, \ell'^-\bar{\nu}_{\ell'}\bar{b}$. The lepton momentum directions $\hat{\mathbf{q}}_\pm$ and the normalized lepton energies $y_\pm = 2E_\pm/m_t$ are defined in the t and $\bar{t}$ rest systems, respectively. The minimal value of the normalized lepton energies is $\mu = m_W^2/m_t^2$. Furthermore $\beta = (1 - 4m_t^2/\hat{s})^{1/2}$ with the parton c.m. energy $\hat{s} = x_1x_2s$, and $\eta = (1-\mu)^2(1+2\mu)/6$. The coefficients $A^{(\lambda)}$, $B^{(\lambda)}_{\pm i}$, and $C^{(\lambda)}_{ij}$ are given[4] in [10].

Eq. (16) has to be modified in an obvious way if phase-space cuts are imposed. The cuts must be CP-invariant in order to avoid any bias in the evaluation of the expectation values of the observables given below. Without such cuts only $A^{(\lambda)}$ contributes to the rate, while the coefficients $B^{(\lambda)}_{\pm i}$ and $C^{(\lambda)}_{ij}$ contain all the information about the $t, \bar{t}$ spin-polarizations and spin-spin correlations, respectively.

Expectation values of observables $\mathcal{O}$ are defined as usual by

$$\langle\, \mathcal{O}\, \rangle \;=\; \frac{\int d\sigma\, \mathcal{O}}{\int d\sigma}\;. \tag{17}$$

For the lepton + jets channels (14), (15) a formula analogous to (16) holds. In this case the appropriate decay density matrices must be used in (12). We note in passing that the cross section measure for $p\bar{p}$ collisions is simply obtained from Eq. (16) by substituting the parton distribution function $N_{\bar{\lambda}}(x_2)$ for $\bar{N}_{\bar{\lambda}}(x_2)$.

Let us now define appropriate angular correlations and asymmetries with which Higgs sector CP violation can be traced in the dilepton and single-lepton channels. Suffice it to say that these correlations and asymmetries can of course be used as tools to search for CP violation in future data independent of any model. If both t and $\bar{t}$ quark decay into semileptonic final states we consider the two observables

$$Q_1 \;\;=\;\; \hat{\mathbf{k}}_t \cdot \hat{\mathbf{q}}_+ - \hat{\mathbf{k}}_{\bar{t}} \cdot \hat{\mathbf{q}}_-\;, \tag{18}$$

and

$$Q_2 \;\;=\;\; (\hat{\mathbf{k}}_t - \hat{\mathbf{k}}_{\bar{t}}) \cdot (\hat{\mathbf{q}}_- \times \hat{\mathbf{q}}_+)/2\;, \tag{19}$$

where $\hat{\mathbf{k}}_t$, $\hat{\mathbf{k}}_{\bar{t}}$ are the t, $\bar{t}$ momentum directions in the parton c.m.s. and $\hat{\mathbf{q}}_+$,$\hat{\mathbf{q}}_-$ are the ℓ^+, ℓ^- momentum directions in the t and $\bar{t}$ quark rest frames, respectively. The channels ℓ^+, ℓ'^- with $\ell, \ell' = e, \mu$ are summed over. Obviously, (18) and (19) are the transcriptions of (6) and (8) to the level of the final states, i.e. (18) and (19) serve as absorptive and dispersive CP observables, respectively, taking account of the fact that the charged lepton is the most efficient analyser of the top-quark spin.

The reconstruction of the t and $\bar{t}$ directions of flight (up to ambiguities) in these channels is possible by solving kinematic constraints [18]. Nevertheless, the measurement of these correlations will be a challenging task. Therefore, we define also corresponding

[4]There are some misprints in the appendix of [10]: in the formula for Γ_Z in Eq. (A10) the denominator should read 32π and the signs of $c_{g1}^{1(f)}, c_{g2}^{1(f)}$ in Eqs. (A21) and (A24) are to be changed.

asymmetries which should be experimentally more robust than (18), (19), because only the signs of Q_1, Q_2 have to be measured, as follows

$$\begin{aligned} A(Q_1) &= \frac{N_{\ell\ell}(Q_1 > 0) - N_{\ell\ell}(Q_1 < 0)}{N_{\ell\ell}} \ , \\ A(Q_2) &= \frac{N_{\ell\ell}(Q_2 > 0) - N_{\ell\ell}(Q_2 < 0)}{N_{\ell\ell}} \ . \end{aligned} \tag{20}$$

$N_{\ell\ell}$ is the number of $t\bar{t}$ events decaying into the dilepton + jets channels. If no phase-space cuts – besides possible cuts on the $t\bar{t}$ invariant mass – are imposed the following relations can be derived between the asymmetries and the expectation values of the corresponding observables:

$$\begin{aligned} A(Q_1) &= \langle\, Q_1 \,\rangle_{\ell\ell} \ , \\ A(Q_2) &= \frac{9\pi}{16} \langle\, Q_2 \,\rangle_{\ell\ell} \ , \end{aligned} \tag{21}$$

where the index $\ell\ell$ refers to the dilepton + jets sample. For the lepton + jets channels we propose the following observables: for sample $\mathcal{A}$ we define

$$O_1 = \hat{\mathbf{k}}_t \cdot \hat{\mathbf{q}}_+ \ , \tag{22}$$

$$O_2 = \hat{\mathbf{k}}_t \cdot (\hat{\mathbf{q}}_+ \times \hat{\mathbf{q}}_{\bar{b}}) \ , \tag{23}$$

where $\hat{\mathbf{q}}_{\bar{b}}$ is the momentum direction of the $\bar{b}$ quark jet in the $\bar{t}$ quark rest frame, while for the sample $\bar{\mathcal{A}}$ we use the charge-conjugated observables

$$\bar{O}_1 = \hat{\mathbf{k}}_{\bar{t}} \cdot \hat{\mathbf{q}}_- \ , \tag{24}$$

$$\bar{O}_2 = \hat{\mathbf{k}}_{\bar{t}} \cdot (\hat{\mathbf{q}}_- \times \hat{\mathbf{q}}_b) \ , \tag{25}$$

with $\hat{\mathbf{q}}_b$ denoting the momentum direction of the b quark jet in the t quark rest frame. In these channels the t and $\bar{t}$ momenta can be reconstructed up to a twofold ambiguity [51]. Taking both samples one can define the quantities

$$\mathcal{E}_1 = \langle\, O_1 \,\rangle_{\mathcal{A}} - \langle\, \bar{O}_1 \,\rangle_{\bar{\mathcal{A}}} \ , \tag{26}$$

$$\mathcal{E}_2 = \langle\, O_2 \,\rangle_{\mathcal{A}} + \langle\, \bar{O}_2 \,\rangle_{\bar{\mathcal{A}}} \ . \tag{27}$$

Eq. (26) is a transcription of the absorptive CP-odd observable (6). The dispersive spin-spin correlation observable (8) implies that in the non-leptonic decay mode of the top quark either the W boson or the b quark jet must act as t-spin analyser. In either case this costs a dilution factor $\kappa \approx 0.41$ (see section 3) – although one gains in statistics as compared with the dilepton channels. For definiteness we have chosen observables that involve the b and $\bar{b}$ jet direction. If reconstruction of the W direction of flight in non-leptonic top quark decays should turn out to be more efficient experimentally, then one should use observables with $\hat{\mathbf{q}}_{\bar{b}} \to -\hat{\mathbf{q}}_{W^-}$ and $\hat{\mathbf{q}}_b \to -\hat{\mathbf{q}}_{W^+}$ in (23), (25). The results given below apply to both cases.

In addition we define corresponding asymmetries as follows

$$\begin{aligned} A(\mathcal{E}_1) &= \frac{N_{\mathcal{A}}(O_1>0)-N_{\mathcal{A}}(O_1<0)}{N_{\mathcal{A}}} - \frac{N_{\bar{\mathcal{A}}}(\bar{O}_1>0)-N_{\bar{\mathcal{A}}}(\bar{O}_1<0)}{N_{\bar{\mathcal{A}}}} \ , \\ A(\mathcal{E}_2) &= \frac{N_{\mathcal{A}}(O_2>0)-N_{\mathcal{A}}(O_2<0)}{N_{\mathcal{A}}} + \frac{N_{\bar{\mathcal{A}}}(\bar{O}_2>0)-N_{\bar{\mathcal{A}}}(\bar{O}_2<0)}{N_{\bar{\mathcal{A}}}} \ . \end{aligned} \tag{28}$$

Here $N_{\mathcal{A}}$ ($N_{\bar{\mathcal{A}}}$) is the number of $t\bar{t}$ events in sample $\mathcal{A}$ ($\bar{\mathcal{A}}$). If no cuts – besides possible cuts on the $t\bar{t}$ invariant mass – are imposed we derive the following relations:

$$\begin{aligned} \mathcal{E}_1 &= \langle\, Q_1 \,\rangle_{\ell\ell} \ , \\ \mathcal{E}_2 &= 2\kappa \,\langle\, Q_2 \,\rangle_{\ell\ell} \ , \end{aligned} \tag{29}$$

and

$$\begin{aligned} A(\mathcal{E}_1) &= \frac{3}{2}\,\mathcal{E}_1 \ , \\ A(\mathcal{E}_2) &= \frac{9\pi}{16}\,\mathcal{E}_2 \ . \end{aligned} \tag{30}$$

Although an a priori classification of observables with respect to CP cannot be made in the case at hand because the initial pp state is not a CP eigenstate, our observables and asymmetries are, nevertheless, good indicators of CP violation for the reactions $pp \to t\bar{t}X \to f_1 f_2 X$ above. The analysis of possible contaminations from CP-invariant interactions which was made in [10] for CP observables that involve momenta defined in the laboratory frame can be applied in an analogous fashion also to the above observables. Here we find that, within the parton model, contributions from CP-invariant interactions to the reactions $gg \to t\bar{t} \to f_1 f_2$ and $q\bar{q} \to t\bar{t} \to f_1 f_2$, i.e. the CP-invariant part of the differential distributions Tr $[\rho^{(f_1)} R^{(\lambda)} \rho^{(f_2)}]$, cannot generate non-zero expectation values of our CP observables. This statement holds to all orders in perturbation theory and can be shown in a straightforward fashion by writing down the expectation values of Q_1, Q_2, using the phase-space measure (16) and using the transformation properties with respect to CP of the coefficients of the production and decay density matrices [10, 45]. An analogous exercise can be performed for $\mathcal{E}_1$, $\mathcal{E}_2$. Kinematic cuts must be CP-invariant.

Moreover, we remark that the T-odd observable (19) and the quantity $\mathcal{E}_2$ are predominantly sensitive to CP violation in the $t\bar{t}$ production amplitude. Possible CP-violating form factors in the amplitudes of the above t and $\bar{t}$ decay channels do not contribute to leading order in the couplings. In order to show this we first note that the above CP observables involve only the momentum of one final-state particle r ($r = \ell, b, W$) from t and/or $\bar{t}$ decay. Then the corresponding decay density matrices are of the form

$$\begin{aligned} \rho^{(f)} &= (\alpha_+ \mathbb{1} + \beta_+ \boldsymbol{\sigma}\cdot\hat{\mathbf{q}}_r) \ , \\ \rho^{(\bar{f})} &= (\alpha_- \mathbb{1} - \beta_- \boldsymbol{\sigma}\cdot\hat{\mathbf{q}}_{\bar{r}}) \ . \end{aligned} \tag{31}$$

CP invariance implies that $\alpha_+ = \alpha_-$, $\beta_+ = \beta_-$. Let us neglect, for a moment, contributions to (31) from absorptive parts of the decay amplitudes. Then CPT invariance enforces the

same conditions on the coefficients $\alpha_\pm, \beta_\pm$ [45]. In other words, there are no contributions to (31) from CP-violating dispersive terms in the decay amplitude if the interactions are CPT invariant. There can be contributions to (31) from CP-violating absorptive parts to one-loop order. However, for CP-violating neutral φ exchange they are absent in the limit of vanishing b quark mass. In supersymmetric models CP-violating gluino, neutralino, and chargino exchange leads to such absorptive parts in the $t \to Wb$ amplitude if $m_t > m_\chi + m_{\tilde{q}}$, where $m_\chi, m_{\tilde{q}}$ denote the masses of a gluino or neutralino and scalar top quark, or those of a chargino and scalar b quark, respectively [42, 24].

In the following $D = \rho^{(f)} \otimes \rho^{(\bar{f})}$ and the labels $disp$ (abs) and I (CP) denote the dispersive (absorptive) parts of the CP-invariant (-violating) terms in the production and decay density matrices, respectively. The T-odd observables $\langle\, Q_2 \,\rangle$, $A(Q_2)$, $\mathcal{E}_2$, and $A(\mathcal{E}_2)$ are generated by the terms

$$\mathrm{Tr}[R_{CP}^{disp} D_I^{disp} + R_I^{disp} D_{CP}^{disp} + R_{CP}^{abs} D_I^{abs} + R_I^{abs} D_{CP}^{abs}] \tag{32}$$

in the squared matrix elements (12) while the T-even observables $\langle\, Q_1 \,\rangle$, $A(Q_1)$, $\mathcal{E}_1$, and $A(\mathcal{E}_1)$ pick up the terms

$$\mathrm{Tr}[R_{CP}^{abs} D_I^{disp} + R_I^{abs} D_{CP}^{disp} + R_{CP}^{disp} D_I^{abs} + R_I^{disp} D_{CP}^{abs}]\,. \tag{33}$$

It remains to count powers of couplings in these expressions. We distinguish between two situations:
(a) For a light φ boson the terms $R_I^{disp}, R_I^{abs}, R_{CP}^{disp}$, and R_{CP}^{abs} are in our normalization of the order $g_s^4, g_s^6/16\pi, g_s^4\lambda_{CP}/16\pi^2$, and $g_s^4\lambda_{CP}/16\pi$, respectively. Here g_s denotes the QCD coupling and λ_{CP} is either γ_{CP} in the case of CP-violating φ exchange or $\mathrm{Im}(g_1 g_2^*)$, where g_1, g_2 denote couplings associated with CP-violating gluino, neutralino, or chargino exchange. The terms D_I^{disp} and D_I^{abs} are of order 1 and $g_s^2/16\pi$, respectively. Further, $D_{CP}^{disp} = 0$. As to D_{CP}^{abs}, it is negligible in the two-Higgs doublet models of section 2 and is of the order $\mathrm{Im}(g_1 g_2^*)/16\pi$ in supersymmetric models. Hence for T-odd observables the first term in (32) is the dominant one. Our argumentation applies to any other theory for which perturbation theory is applicable. This proves the above statement. For T-even observables the first and the last term in (33) are in general – apart from the two-Higgs doublet models in section 2 – of the same order of magnitude.
(b) For a heavy φ boson with mass $m_\varphi > 2m_t$, where the dominant contribution to R_{CP} in the resonance region $|\hat{s} - m_\varphi^2| \lesssim m_\varphi \Gamma_\varphi$ comes from $gg \to \varphi \to t\bar{t}$, the situation is the following. Using the formula for $\Gamma_\varphi = \Gamma_W + \Gamma_Z + \Gamma_t$ (see Eq. (48) of the appendix) and assuming that the reduced Yukawa couplings $a, \tilde{a}$ are of order 1, the inspection of the s-channel contribution yields that now R_{CP}^{disp} and R_{CP}^{abs} are of order g_s^4 and g_s^4/π, respectively, while R_I^{disp}, R_I^{abs} are of the same order as above. (Actually, CP-invariant s-channel φ exchange is also relevant to these terms.) In this case, both in (32) and in (33), the first terms are the dominant ones. Thus for a heavy φ boson all the CP observables defined above are predominantly sensitive to CP violation in $gg \to \varphi \to t\bar{t}$.

It is clear that, especially in the case of resonant φ production, the sensitivity of the above observables to a non-zero product γ_{CP} of Yukawa couplings can be enhanced considerably by judicious choices of cuts on the invariant $t\bar{t}$ mass $M_{t\bar{t}} = \sqrt{(k_t + k_{\bar{t}})^2}$. In

fact such a cut is mandatory in view of the remarks made at the end of section 2. The spectrum $d\sigma/dM_{t\bar{t}}$ is obtained by multiplying the cross sections $\int d\hat{\sigma}^{(\lambda)}$ for the parton subprocesses at $\hat{s} = M_{t\bar{t}}^2$ with the so-called luminosity functions

$$L^{(\lambda)}(\tau) = 2\tau \int_\tau^{1/\tau} \frac{d\zeta}{\zeta} N_\lambda(\tau\zeta) N_{\bar{\lambda}}(\frac{\tau}{\zeta}) \ , \tag{34}$$

where $\tau = M_{t\bar{t}}/\sqrt{s}$. That is, one has

$$\frac{d\sigma}{dM_{t\bar{t}}} = \frac{1}{\sqrt{s}} \sum_\lambda L^{(\lambda)}(M_{t\bar{t}}/\sqrt{s}) \int d\hat{\sigma}^{(\lambda)}(M_{t\bar{t}}^2) \ . \tag{35}$$

Let us define a "differential expectation value" $\prec\mathcal{O}\succ$ for a given invariant $t\bar{t}$ mass by

$$\prec\mathcal{O}\succ(M_{t\bar{t}}) \equiv \frac{\langle\, \mathcal{O}\delta(\sqrt{\hat{s}} - M_{t\bar{t}})\,\rangle}{\langle\, \delta(\sqrt{\hat{s}} - M_{t\bar{t}})\,\rangle} = \frac{\displaystyle\sum_\lambda L^{(\lambda)}(M_{t\bar{t}}/\sqrt{s}) \int d\hat{\sigma}^{(\lambda)}(M_{t\bar{t}}^2)\, \mathcal{O}}{\displaystyle\sum_\lambda L^{(\lambda)}(M_{t\bar{t}}/\sqrt{s}) \int d\hat{\sigma}^{(\lambda)}(M_{t\bar{t}}^2)} \ . \tag{36}$$

These quantities, which we shall compute in the next section for the observables $Q_{1,2}$, turn out to be very good indicators of how to choose appropriate $M_{t\bar{t}}$ mass bins for the evaluation of the expectation values and asymmetries of the above observables.

5 Results

Throughout this section we put $m_t = 175$ GeV and $m_W = 80.4$ GeV. In the computations we took the parton distribution functions (PDF) from [52], evaluated at the factorization scale $\Lambda = 2m_t$, and convinced ourselves that our results do not change significantly if we vary Λ or work with other PDF sets [53]. Furthermore all sensitivity estimates are based on an LHC integrated luminosity of 100 fb^{-1} at $\sqrt{s} = 14$ TeV.

Let us first assess the relative size of the $gg \to \varphi \to t\bar{t}$ (which we call resonant) and the remaining φ contributions (which we call non-resonant) to $t\bar{t}$ production. As already emphasized, all the interferences with the non-resonant QCD background are included. For this purpose we have plotted in Figs. 1 and 2 the resonant and all φ contributions to the differential expectation values (36) of Q_1 and Q_2 as a function of the $t\bar{t}$ invariant mass $M_{t\bar{t}}$ for four different Higgs boson masses. Figs. 1 and 2 illustrate the fact that for $m_\varphi > 2m_t$ the non-resonant contributions are negligible with respect to the s-channel φ contribution. Therefore we take the non-resonant terms into account only when evaluating observables for $m_\varphi \leq 2m_t$.

In Figs. 3 – 7 we show again the values of $\prec Q_1\succ$ and $\prec Q_2\succ$ as a function of $M_{t\bar{t}}$; this time for Higgs boson masses $m_\varphi \geq 2m_t$ and for different values of the couplings g_{VV}, a, and $\tilde{a}$. Only the resonant φ contributions are included. The figures show the characteristic peak-dip structure in the resonance region. The height and the width of the peaks depend on the Higgs boson decay width Γ_φ and on its Yukawa couplings to

top quarks. As usual the peaks get broader and less pronounced with increasing Γ_φ. As expected, the height of a peak is, for a given φ mass and set of couplings, larger for Q_2 than for Q_1. Note that in the resonance region the sensitivity of these observables to γ_{CP} is high.

These plots can be used to choose appropriate $M_{t\bar{t}}$ mass bins for the evaluation of the CP observables and asymmetries on the dilepton and the lepton + jets samples. The peak-dip structure of the signals in Figs. 3 – 7 suggests to select, for a "known" Higgs boson mass, $M_{t\bar{t}}$ mass bins below (if kinematically possible) and above m_φ. Our choices are given in Table 1 and will be used below.

In addition we shall apply further cuts, namely

$$|y(t)| \leq 3 \,, \qquad p_T \geq 20\,\mathrm{GeV} \tag{37}$$

for the rapidities of the t and $\bar{t}$ quarks and for the transverse momenta in the laboratory frame of the final-state charged leptons and quarks in the dilepton and the lepton + jets samples.

Implementing (37) and the $M_{t\bar{t}}$ intervals of Table 1 in the cross section measure (16) and in the analogous measure for the lepton + jets channels, we have numerically computed $\langle\, Q_1 \,\rangle$, $\langle\, Q_2 \,\rangle$, $\mathcal{E}_1$, and $\mathcal{E}_2$. In the same way we have computed the 1 s.d. statistical errors $\delta\mathcal{O} = [(\langle\, \mathcal{O}^2 \,\rangle - \langle\, \mathcal{O} \,\rangle^2)/N]^{1/2}$ of the CP observables $\mathcal{O}$. Here N is the number of events in the respective sample and $M_{t\bar{t}}$ interval that pass the above cuts. We considered Higgs boson masses and reduced couplings in the ranges 320 GeV $\leq m_\varphi \leq$ 500 GeV, 0.3 $\leq |a|, |\tilde{a}| \leq 1$, $|g_{VV}| \leq 0.4$. Without loss of generality the signs of $a, \tilde{a}$ were chosen such that $\gamma_{CP} > 0$.

The results are given in Tables 2 – 9. The non-resonant contributions have been included only for $m_\varphi = 320$ GeV and $m_\varphi = 350$ GeV. For each value of $m_\varphi, g_{VV}, a, \tilde{a}$ the number in the first column of the respective sub-table contains the expectation value in percent and the second number is the statistical significance (in s.d.) of the CP effect for 100 fb^{-1} of integrated LHC luminosity. Tables 2 – 5 show that the dispersive observable Q_2 has a higher sensitivity to Higgs sector CP violation than the absorptive observable Q_1. The sensitivities of $\mathcal{E}_1$ and $\mathcal{E}_2$ are, by and large, of the same order. (Recall that the quality of $\mathcal{E}_2$ is diminished with respect to $\langle\, Q_2 \,\rangle$ because of the limited t-spin analysing power of the b quark jet.)

These investigations can be extended to the channels where both t and $\bar{t}$ decay non-leptonically. In this case one may use observables which result from replacing $\hat{\mathbf{q}}_+, \hat{\mathbf{q}}_- \to \hat{\mathbf{q}}_b, \hat{\mathbf{q}}_{\bar{b}}$ in (18), (19).

In this context another relevant observable is the $t\bar{t}$ spin-spin correlation $\mathbf{s}_t \cdot \mathbf{s}_{\bar{t}}$, which translates into

$$Q_3 \;=\; \hat{\mathbf{q}}_+ \cdot \hat{\mathbf{q}}_- \,, \tag{38}$$

for the dilepton sample (13), where $\hat{\mathbf{q}}_+, \hat{\mathbf{q}}_-$ are the ℓ^+, ℓ^- momenta as defined above. Although $\mathbf{s}_t \cdot \mathbf{s}_{\bar{t}}$ and (38) are not proportional to γ_{CP}, they are sensitive to the Yukawa couplings $a, \tilde{a}$ [12] and should therefore also be measured in future experiments. The expectation value $\langle\, Q_3 \,\rangle$ was computed in terms of a and $\tilde{a}$ in [34].

The amount of numerical work can be drastically simplified if no cuts besides the one on $M_{t\bar{t}}$ are imposed. In this case we can derive a formula that allows for a rather fast computation of the expectation values $\langle\, Q_{1,2}\,\rangle$ for the dilepton samples. It is given in the appendix and we also give there the widths of the distributions of the CP observables. We have found that the results for the expectation values and statistical sensitivities obtained in this way differ only slightly from the ones presented in Tables 2 – 9.

The asymmetries $A(Q_{1,2})$ and the quantities $\mathcal{E}_{1,2}$ and $A(\mathcal{E}_{1,2})$ for the lepton + jets sample are determined in this case by the general relations given in section 4. With these formulae we can easily compute the CP asymmetries and the statistical sensitivities $|\langle\, Q_1\,\rangle|/\delta Q_1$, etc.. By comparing these numbers we find that the sensitivities of $Q_1, Q_2, \mathcal{E}_1$, and $\mathcal{E}_2$ are larger by about 20% than those for $A(Q_1), A(Q_2), A(\mathcal{E}_1)$, and $A(\mathcal{E}_2)$, respectively. On the other hand, as mentioned, the asymmetries should be experimentally more robust.

With the above results we conclude that for a large range of φ masses values of $|\gamma_{CP}| \gtrsim 0.1$ can be traced with the observables of section 4. As far as we can see it is, in the foreseeable future, a rather unique possibility of the LHC to make CP tests for heavy Higgs bosons. In view of this opportunity analyses of hadronization and detector effects on the sensitivities of these observables, which are beyond the scope of this paper, would be worthwhile.

We close with two remarks. In [10] "experimentally simple" CP observables involving momenta in the laboratory frame were studied. Moreover, no cuts on $M_{t\bar{t}}$ were made. Therefore these observables are considerably less sensitive to γ_{CP} than those of section 4. In [15] so-called optimal CP observables – which are essentially given by the CP-violating terms in the squared matrix element divided by its CP-invariant part – were considered (without $M_{t\bar{t}}$ cuts) and found to be sensitive to $|\gamma_{CP}| \gtrsim 0.1$. While the construction and evaluation of optimal CP observables is straightforward theoretically [54], their experimental usefulness in the case at hand remains to be seen: apart from depending on many kinematic variables they involve also model-dependent parameters, in particular particle masses, which may be unknown.

6 Conclusions

In several extensions of the SM the Higgs sector can, apart from breaking the electroweak gauge symmetry, also violate CP. The neutral Higgs bosons φ which are predicted by these models then act also as messengers of the latter phenomenon. In this paper we have shown that top-quark pair production at the LHC offers a good possibility to investigate whether or not the interactions of neutral Higgs bosons are CP-violating. The observables and asymmetries that we have proposed and investigated were found to be very sensitive to the product of scalar and pseudoscalar top-quark Yukawa couplings, namely $|\gamma_{CP}| \gtrsim 0.1$. At least as far as heavy Higgs bosons are concerned, these would be rather unique CP tests in the foreseeable future.

Acknowledgments

We thank W. Hollik and H. Y. Zhou for discussions. W.B. wishes to thank the Theory Division at CERN for the hospitality extended to him.

Appendix

In this appendix we give a compact formula for the expectation values of the observables defined in section 4, which allows for a rather quick evaluation.

When no cuts are applied, the multiple phase-space integrals that appear in (17) can be performed up to the two-dimensional integrals over the momentum fractions x_1, x_2 of the colliding partons in the initial state. Here we consider a neutral φ boson with mass $m_\varphi \geq 2m_t$, which is the most interesting case. Then the CP-violating φ contribution to $t\bar{t}$ production is dominated by the s-channel $gg \to \varphi \to t\bar{t}$ diagram, and the other non-resonant φ contributions of order γ_{CP} to $gg, q\bar{q} \to t\bar{t}$ can be neglected as shown in section 5.

For the dilepton channels (13) we find for the expectation values of the observables (18), (19):

$$\langle\, Q_1 \,\rangle_{\ell\ell} = \frac{2}{3}\,\mathcal{F}[B]\;, \quad \langle\, Q_2 \,\rangle_{\ell\ell} = \frac{2}{9}\,\mathcal{F}[C]\;, \tag{39}$$

where $\mathcal{F}[G]$ denotes the ratio of integrals

$$\begin{aligned}
\mathcal{F}[G] &= \frac{\displaystyle\int_0^1 dx_1 \int_0^1 dx_2\, \Theta(\hat{s}-4m_t^2)\;\beta/\hat{s}\;\sum_\lambda N_\lambda(x_1) N_{\bar{\lambda}}(x_2)\, G^{(\lambda)}(\hat{s})}{\displaystyle\int_0^1 dx_1 \int_0^1 dx_2\, \Theta(\hat{s}-4m_t^2)\;\beta/\hat{s}\;\sum_\lambda N_\lambda(x_1) N_{\bar{\lambda}}(x_2)\, W^{(\lambda)}(\hat{s})} \\
&= \frac{\displaystyle\int_r^1 d\tau\, \beta/\hat{s} \sum_\lambda L^{(\lambda)}(\tau) G^{(\lambda)}(\hat{s})}{\displaystyle\int_r^1 d\tau\, \beta/\hat{s} \sum_\lambda L^{(\lambda)}(\tau) W^{(\lambda)}(\hat{s})}\;.
\end{aligned} \tag{40}$$

Here $N_\lambda(x_1)$, $N_{\bar{\lambda}}(x_2)$ denote the parton distribution functions, $L^{(\lambda)}$ is the luminosity function defined in Eq. (34), $\tau = \sqrt{\hat{s}/s}$ and $r = 2m_t/\sqrt{s}$. The functions $B^{(\lambda)}, C^{(\lambda)}$ and $W^{(\lambda)}$ are given below.

If the expectation values Eq. (39) are evaluated for events in a given $M_{t\bar{t}}$ bin, $M_{t\bar{t}} = \sqrt{\hat{s}} \in [M_{\rm low}, M_{\rm high}]$, the factor $\Theta(\sqrt{\hat{s}} - M_{\rm low})\Theta(M_{\rm high} - \sqrt{\hat{s}})$ has to be inserted in all the integrals of Eq. (40).

The quantities $\mathcal{E}_{1,2}$ defined in Eqs. (26), (27) and the asymmetries defined in Eqs. (20) and (28) can then also be calculated with the formulae (39) using the relations (29), (21), and (30) respectively.

In order to estimate the statistical sensitivity of the observables $Q_{1,2}$ to Higgs sector CP violation, we need also the widths of the distributions of these observables, i.e. the expectation values of their squares. We find that

$$\langle\, Q_1^2 \,\rangle_{\ell\ell} = \frac{2}{3} - \frac{2}{9}\,\mathcal{F}[D]\;, \quad \langle\, Q_2^2 \,\rangle_{\ell\ell} = \frac{2}{9}\;. \tag{41}$$

As usual, the widths are given by

$$\Delta Q_i = \sqrt{\langle\, Q_i^2 \,\rangle_{\ell\ell} - \langle\, Q_i \,\rangle_{\ell\ell}^2}\;. \tag{42}$$

For the single lepton channels (14), (15) we find that

$$\langle O_1^2 \rangle_{\mathcal{A}} = \langle \bar{O}_1^2 \rangle_{\bar{\mathcal{A}}} = \frac{1}{3} \,, \quad \langle O_2^2 \rangle_{\mathcal{A}} = \langle \bar{O}_2^2 \rangle_{\bar{\mathcal{A}}} = \frac{2}{9} \,, \tag{43}$$

and the widths are given by $\Delta O_i = (\langle O_i^2 \rangle_{\mathcal{A}} - \langle O_i \rangle_{\mathcal{A}}^2)^{1/2}$, $\Delta \bar{O}_i = \left(\langle \bar{O}_i^2 \rangle_{\bar{\mathcal{A}}} - \langle \bar{O}_i \rangle_{\bar{\mathcal{A}}}^2\right)^{1/2}$. Note that the above results also hold for individual bins in $M_{t\bar{t}}$.
The functions $G^{(\lambda)} \in \{B^{(\lambda)}, C^{(\lambda)}, D^{(\lambda)}\}$ and $W^{(\lambda)}$ read

$$\begin{aligned}
W^{(q)} &= \frac{2}{9}\left[1 - \frac{1}{3}\beta^2\right] \,, \\
W^{(g)} &= \frac{1}{96}\left[31\beta^2 - 59 - (33 - 18\beta^2 + \beta^4)\frac{\ln(\omega)}{\beta}\right] \\
&\quad - K\,\frac{x^2}{16}\left[\beta^2 a^2 \mathrm{Re}(d) + \tilde{a}^2 \mathrm{Re}(\tilde{d})\right]\frac{\ln(\omega)}{\beta} \\
&\quad + K^2\,\frac{3x^2}{16}(\beta^2 a^2 + \tilde{a}^2)\left(a^2|d|^2 + \tilde{a}^2|\tilde{d}|^2\right) \,, \\
B^{(g)} &= -K\,\frac{x^2}{16}\; a\tilde{a}\;\mathrm{Im}(d - \tilde{d})\ln(\omega) \,, \\
C^{(g)} &= K\,\frac{x^2}{16}\; a\tilde{a}\left[\mathrm{Re}(d + \tilde{d})\ln(\omega) - 6K\beta\left(a^2|d|^2 + \tilde{a}^2|\tilde{d}|^2\right)\right] \,, \\
D^{(q)} &= \frac{2}{27}(1 + \beta^2) \,, \\
D^{(g)} &= \frac{1}{96\beta^2}\left[(\beta^6 - 17\beta^4 + 33\beta^2 - 33)\frac{\ln(\omega)}{\beta} - (31\beta^4 - 37\beta^2 + 66)\right] \\
&\quad + K\,\frac{x^2}{16}\left[\beta^2 a^2 \mathrm{Re}(d) + \tilde{a}^2 \mathrm{Re}(\tilde{d})\right]\frac{\ln(\omega)}{\beta} \\
&\quad - K^2\,\frac{3x^2}{16}(\beta^2 a^2 + \tilde{a}^2)\left(a^2|d|^2 + \tilde{a}^2|\tilde{d}|^2\right) \,, \\
B^{(q)} &= C^{(q)} = 0 \,.
\end{aligned} \tag{44}$$

where a, $\tilde{a}$ are the reduced top quark Yukawa couplings of Eq. (1),

$$\omega = \frac{1-\beta}{1+\beta} \,, \quad \beta = \sqrt{1 - x^2} \,, \quad x = \frac{2m_t}{\sqrt{\hat{s}}} \,, \quad \hat{s} = x_1 x_2 s \,, \tag{45}$$

and we have used the abbreviations

$$\begin{aligned}
K &= \sqrt{2} G_F \left(\frac{m_t}{4\pi}\right)^2 \,, \\
d &= (-2 + \beta^2 \hat{s} C_0)\frac{\hat{s}}{\hat{s} - m_\varphi^2 + i m_\varphi \Gamma_\varphi} \,, \\
\tilde{d} &= \hat{s} C_0 \frac{\hat{s}}{\hat{s} - m_\varphi^2 + i m_\varphi \Gamma_\varphi} \,,
\end{aligned} \tag{46}$$

with

$$C_0 = \frac{1}{2\hat{s}} \left[\ln(\omega) + i\pi\right]^2 \ , \tag{47}$$

and Γ_φ is the width of φ. As we work to lowest order in the Yukawa couplings we have adopted the energy-independent width approximation for the φ propagator. The width Γ_φ is the sum of partial widths for $\varphi \to W^+W^-, ZZ, t\bar{t}$, i.e., $\Gamma_\varphi = \Gamma_W + \Gamma_Z + \Gamma_t$ with

$$\begin{aligned}
\Gamma_W &= \Theta(m_\varphi - 2m_W) \frac{g_{VV}^2 \sqrt{2} G_F m_\varphi^3 \beta_W}{16\pi} \left[\beta_W^2 + 12 \frac{m_W^4}{m_\varphi^4}\right] , \\
\Gamma_Z &= \Theta(m_\varphi - 2m_Z) \frac{g_{VV}^2 \sqrt{2} G_F m_\varphi^3 \beta_Z}{32\pi} \left[\beta_Z^2 + 12 \frac{m_Z^4}{m_\varphi^4}\right] , \\
\Gamma_t &= \Theta(m_\varphi - 2m_t) \frac{3\sqrt{2} G_F m_\varphi m_t^2 \beta_t}{8\pi} \left[\beta_t^2 a^2 + \tilde{a}^2\right] .
\end{aligned} \tag{48}$$

Here we have used the notation $\beta_{W,Z,t} = \left(1 - 4m_{W,Z,t}^2/m_\varphi^2\right)^{1/2}$.

References

[1] T. D. Lee, Phys. Rev. D8 (1973) 1226; Phys. Rep. C9 (1974) 143.

[2] N. G. Deshpande and E. Ma, Phys. Rev. D16 (1977) 1583.

[3] G. C. Branco and M. N. Rebelo, Phys. Lett. B160 (1985) 117.

[4] J. Liu and L. Wolfenstein, Nucl. Phys. B289 (1987) 1.

[5] S. Weinberg, Phys. Rev. D42 (1990) 860.

[6] M. Matsuda and M. Tanimoto, Phys. Rev. D52 (1995) 3100;
N. Haba, Prog. Theor. Phys. 97 (1997) 301.

[7] K. S. Babu, C. Kolda, J. March-Russell and F. Wilczek, hep-ph/9804355.

[8] A. Pilaftsis, Phys. Lett. B435 (1998) 88.

[9] W. Bernreuther and A. Brandenburg, Phys. Lett. B314 (1993) 104.

[10] W. Bernreuther and A. Brandenburg, Phys. Rev. D49 (1994) 4481.

[11] D. Chang, W. Y. Keung and I. Phillips, Phys. Rev. D48 (1993) 3225.

[12] W. Bernreuther, A. Brandenburg and M. Flesch, Phys. Rev. D56 (1997) 90.

[13] A. Skjold and P. Osland, Phys. Lett. B329 (1994) 305.

[14] C.R. Schmidt and M.E. Peskin, Phys. Rev. Lett. 69 (1992) 410.

[15] H. Y. Zhou, Phys. Rev. D58 (1998) 114002.

[16] X. Zhang et al., Phys. Rev. D50 (1994) 7042;
S. Bar-Shalom et al., Phys. Rev. D53 (1996) 1162;
J. F. Gunion and X. G. He, Phys. Rev. Lett. 76 (1996) 4468.

[17] G. L. Kane, G. A. Ladinsky and C. P. Yuan, Phys. Rev. D45 (1992) 124.

[18] D. Atwood, A. Aeppli and A. Soni, Phys. Rev. Lett. 69 (1992) 2756.

[19] A. Brandenburg and J. P. Ma, Phys. Lett. B298 (1993) 211.

[20] P. Haberl, O. Nachtmann and A. Wilch, Phys. Rev. D53 (1996) 4875.

[21] B. Grzadkowski, B. Lampe and K. J. Abraham, Phys. Lett. B415 (1997) 193.

[22] C. R. Schmidt, Phys. Lett. B293 (1992) 111.

[23] D. Atwood et al., Phys. Rev. D54 (1996) 5412.

[24] S. Bar-Shalom, D. Atwood and A. Soni, Phys. Rev. D57 (1998) 1495.

[25] M. Kobayashi and T. Maskawa, Prog. Theor. Phys. 49 (1973) 652.

[26] W. Bernreuther, T. Schröder and T.N. Pham, Phys. Lett. B279 (1992) 389.

[27] F. M. Borzumati and C. Greub, Phys. Rev. D58 (1998) 074004; hep-ph/9809438.

[28] A. J. Buras, P. Krawczyk, M. E. Lautenbacher and C. Salazar, Nucl. Phys. B337 (1990) 284.

[29] K. F. Smith et al., Phys. Lett. B234 (1990) 191;
I. S. Altarev et al., Phys. Lett. B276 (1992) 242.

[30] E. D. Commins, S. B. Ross, D. DeMille and B. C. Regan, Phys. Rev. A50 (1994) 2960.

[31] T. Hayashi et al., Phys. Lett. B348 (1995) 489.

[32] M. Chemtob, Phys. Rev. D45 (1992) 1649;
J. Ellis and R. Flores, Phys. Lett. B377 (1996) 83;
I. B. Khriplovich, Phys. Lett. B382 (1996) 145.

[33] W. Bernreuther, hep-ph/9808453.

[34] W. Bernreuther, M. Flesch and P. Haberl, Phys. Rev. D58 (1998) 114031.

[35] S. Dawson, A. Djouadi and M. Spira, Phys. Rev. Lett. 77 (1996) 16.

[36] A. Djouadi, M. Spira and P. Zerwas, Phys. Lett. B264 (1991) 440;
D. Graudenz, M. Spira and P. Zerwas, Phys. Rev. Lett. 70 (1993) 1372;
S. Dawson, Nucl. Phys. B359 (1991) 283.

[37] M. Spira, A. Djouadi, D. Graudenz and P. Zerwas, Nucl. Phys. B453 (1995) 17.

[38] M. Krämer, E. Laenen and M. Spira, Nucl. Phys. B511 (1998) 523.

[39] W. Beenakker, A. Denner, W. Hollik, R. Mertig, T. Sack and D. Wackeroth, Nucl. Phys. B411 (1994) 343.

[40] K. Gaemers and F. Hoogeveen, Phys. Lett. B146 (1984) 347.

[41] D. Dicus, A. Stange and S. Willenbrock, Phys. Lett. B333 (1994) 126.

[42] W. Bernreuther and P. Overmann, Z. Phys. C61 (1994) 599.

[43] W. Bernreuther, A. Brandenburg and P. Uwer, Phys. Lett. B368 (1996) 153.

[44] W.G.D. Dharmaratna and G. R. Goldstein, Phys. Rev. D53 (1996) 1073.

[45] W. Bernreuther, O. Nachtmann, P. Overmann and T. Schröder, Nucl. Phys. B388 (1992) 53; B406 (1993) 516 (E).

[46] J. P. Ma and A. Brandenburg, Z. Phys. C56 (1992) 97.

[47] A. Czarnecki, M. Jezabek and J. H. Kühn, Nucl. Phys. B351 (1991) 70.

[48] B. Grzadkowski and J. F. Gunion, Phys. Lett. B287 (1992) 237;
T. Hasuike, T. Hattori and S. Wakaizumi, Phys. Rev. D58 (1998) 095008.

[49] J.A. Coarasa, J. Guasch, J. Sola and W. Hollik, hep-ph/980827.

[50] F. Abe et al. (CDF Collab.), Phys. Rev. Lett. 79 (1997) 357.

[51] G. A. Ladinsky, Phys. Rev. D46 (1992) 3789; D47 (1993) 3086 (E).

[52] M. Glück, E. Reya and A. Vogt, Z. Phys. C67 (1995) 433.

[53] A. D. Martin, W. J. Stirling and R. G. Roberts, Phys. Lett. B354 (1995) 155;
H. L. Lai *et al.* (CTEQ Collab.), Phys. Rev. D51 (1995) 4763.

[54] D. Atwood and A. Soni, Phys. Rev. D45 (1992) 2405;
M. Diehl and O. Nachtmann, Z. Phys. C62 (1994) 397.

Figure Captions

Fig. 1: Differential expectation value of Q_1 (see (36)) at $\sqrt{s} = 14$ TeV for $g_{VV} = 0$, reduced Yukawa couplings $a = 1$, $\tilde{a} = -1$, and Higgs boson masses $m_\varphi = 320$ GeV (a), 350 GeV (b), 400 GeV (c), and 500 GeV (d) in the dilepton channel. The dashed line represents the resonant and the solid line the sum of the resonant and non-resonant φ contributions to $\prec Q_1 \succ$.

Fig. 2: Same as Figure 1 for the observable Q_2.

Fig. 3: Differential expectation value of Q_1 at $\sqrt{s} = 14$ TeV for different Higgs boson masses and couplings a, $\tilde{a}$ and $g_{VV} = 0$ in the dilepton channel. $m_\varphi = 350$ GeV (solid line), $m_\varphi = 370$ GeV (dashed line), $m_\varphi = 400$ GeV (dotted line), $m_\varphi = 500$ GeV (dash-dotted line). Figures a, b, c, d correspond to $(a, \tilde{a}) = (1, -1)$, $(1, -0.3)$, $(0.3, -1)$, $(0.3, -0.3)$. Only the resonant φ contributions are shown.

Fig. 4: Same as Figure 3, but $g_{VV} = 0.4$.

Fig. 5: Same as Figure 3, but observable Q_2.

Fig. 6: Same as Figure 5, but $g_{VV} = 0.4$.

Table Captions

Table 1: Selection of the $M_{t\bar{t}}$ interval below and above a Higgs boson mass m_φ in units of GeV.

Table 2: The expectation value of Q_1 and its sensitivity at $\sqrt{s} = 14$ TeV for the dilepton channels. The $M_{t\bar{t}}$ interval is chosen below m_φ as given in Table 1. For each pair $(m_\varphi,\, g_{VV})$ the first column is $\langle\, Q_1 \,\rangle$ in percent and the second column is the sensitivity in s.d. The rows correspond, in descending order, to $(a,\, \tilde{a})$ $= (1, -1)$, $(1, -0.3)$, $(0.3, -1)$, $(0.3, -0.3)$. Numbers for m_φ are in GeV. The non-resonant contributions have been neglected for these values of m_φ.

Table 3: Same as Table 2, but with $M_{t\bar{t}}$ interval above m_φ as given in Table 1. For $m_\varphi = 320$ GeV and $m_\varphi = 350$ GeV the non-resonant contributions have been included.

Table 4: Same as Table 2 for the expectation value of Q_2.

Table 5: Same as Table 3 for the expectation value of Q_2.

Table 6: Same as Table 2 for the quantity $\mathcal{E}_1$ in the lepton + jets channels.

Table 7: Same as Table 3 for the quantity $\mathcal{E}_1$in the lepton + jets channels.

Table 8: Same as Table 2 for the quantity $\mathcal{E}_2$ in the lepton + jets channels.

Table 9: Same as Table 3 for the quantity $\mathcal{E}_2$ in the lepton + jets channels.

Figures

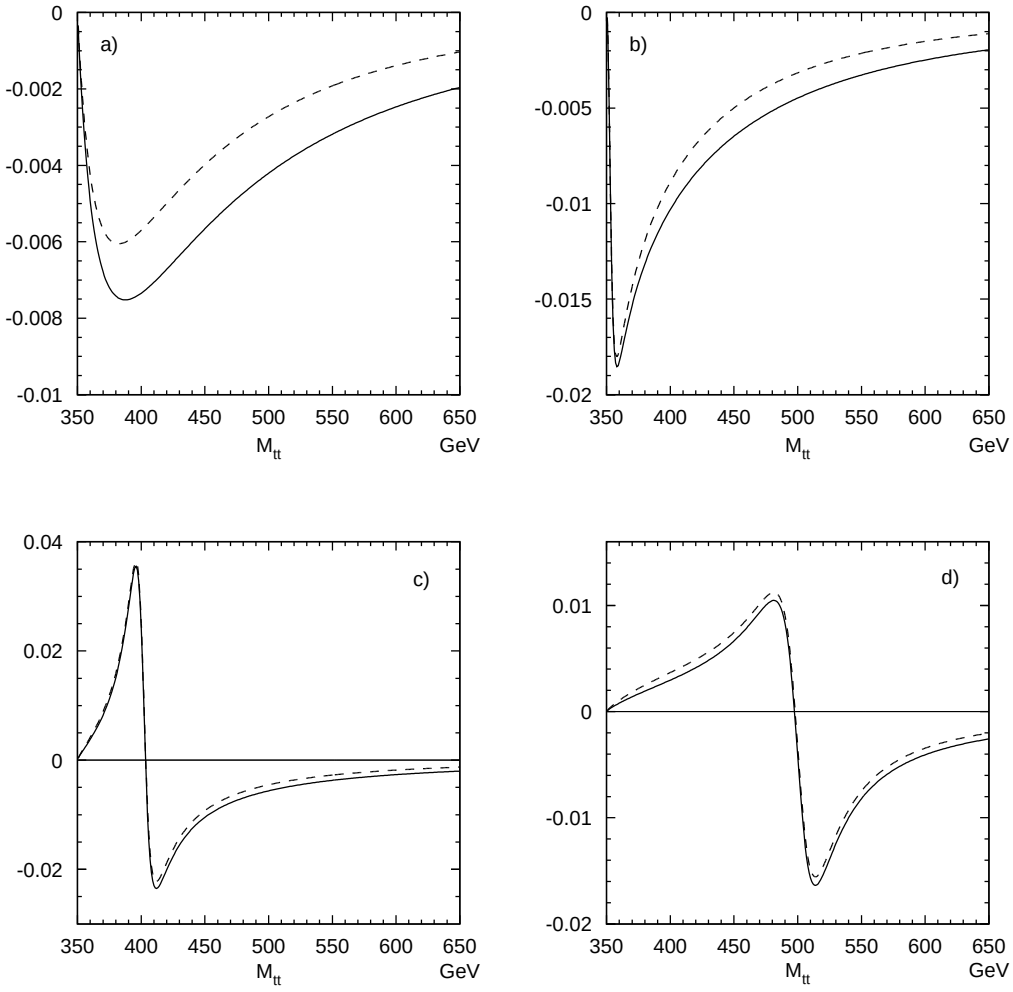

Figure 1

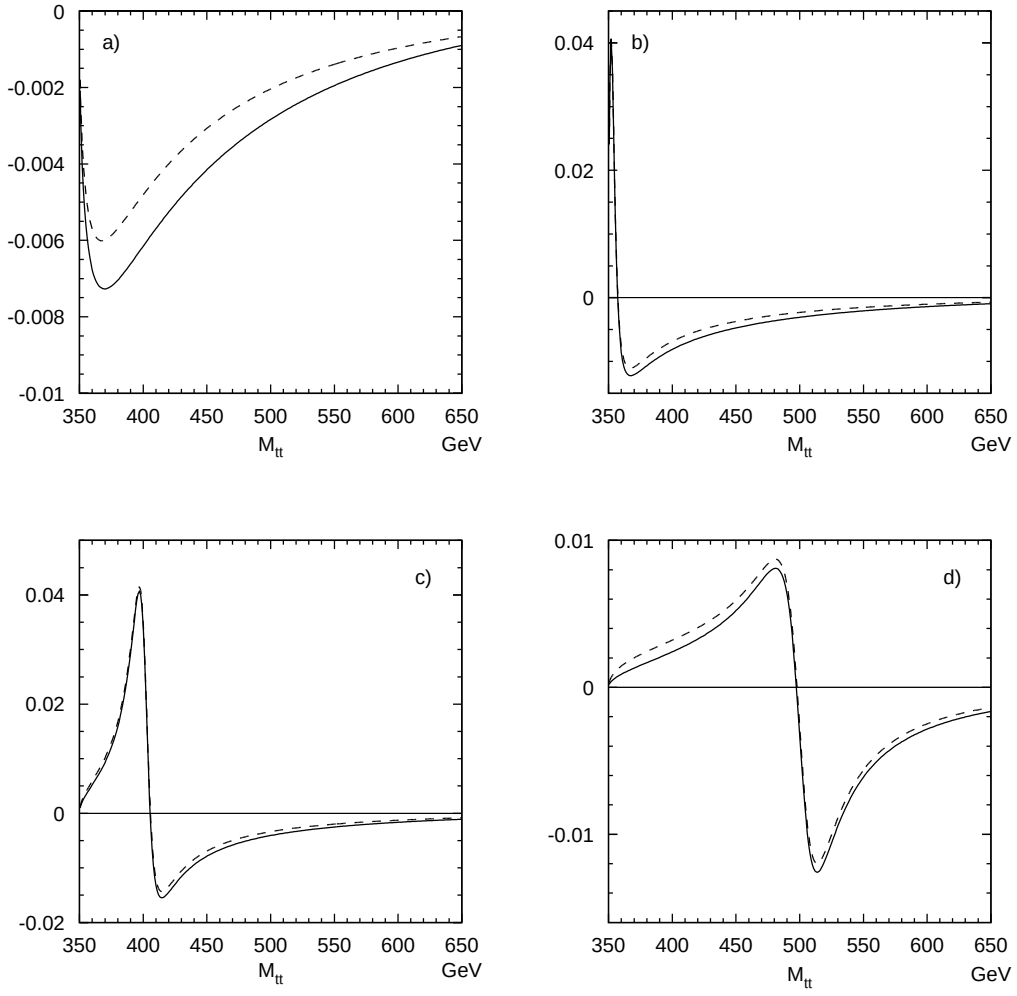
a)
b)
c)
d)
0
-0.002
-0.004
-0.006
-0.008
-0.01
0.04
0.02
0
-0.02
0.01
-0.01
350
400
450
500
550
600
650
M_{tt}
GeV

Figure 2

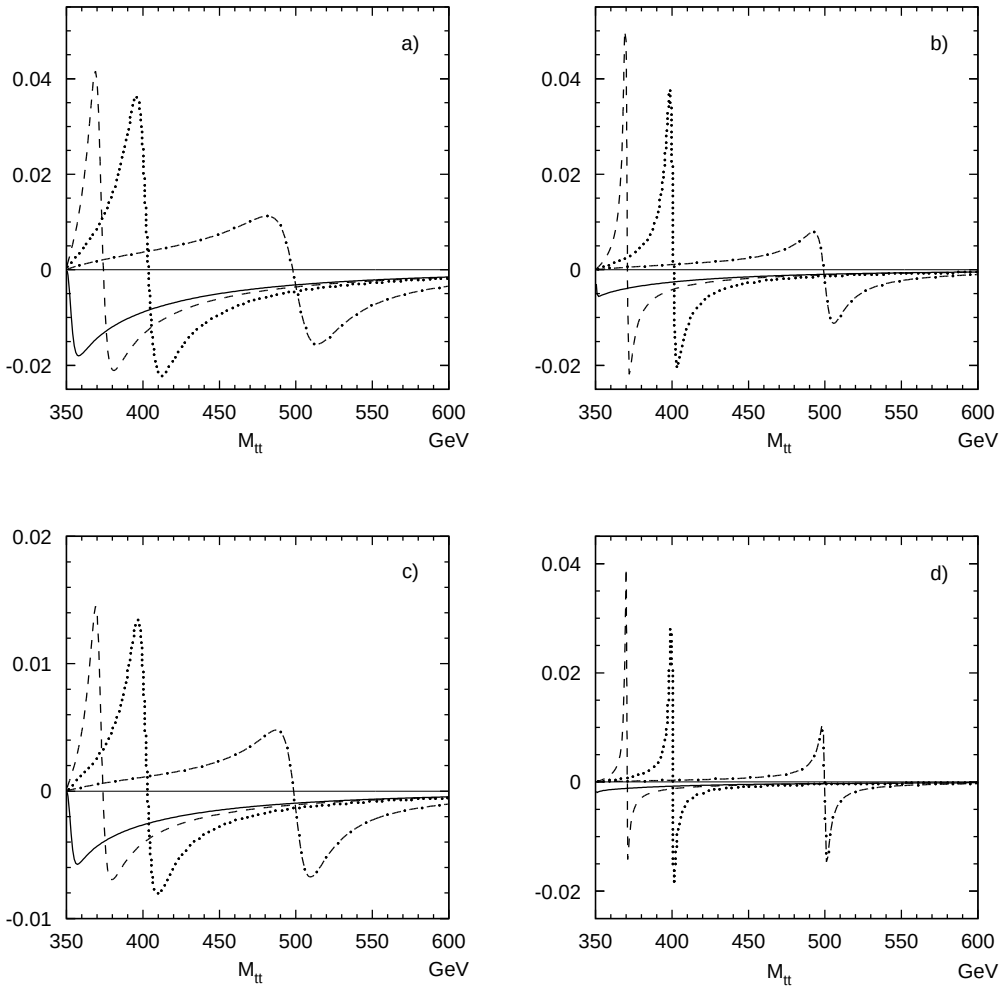

Figure 3

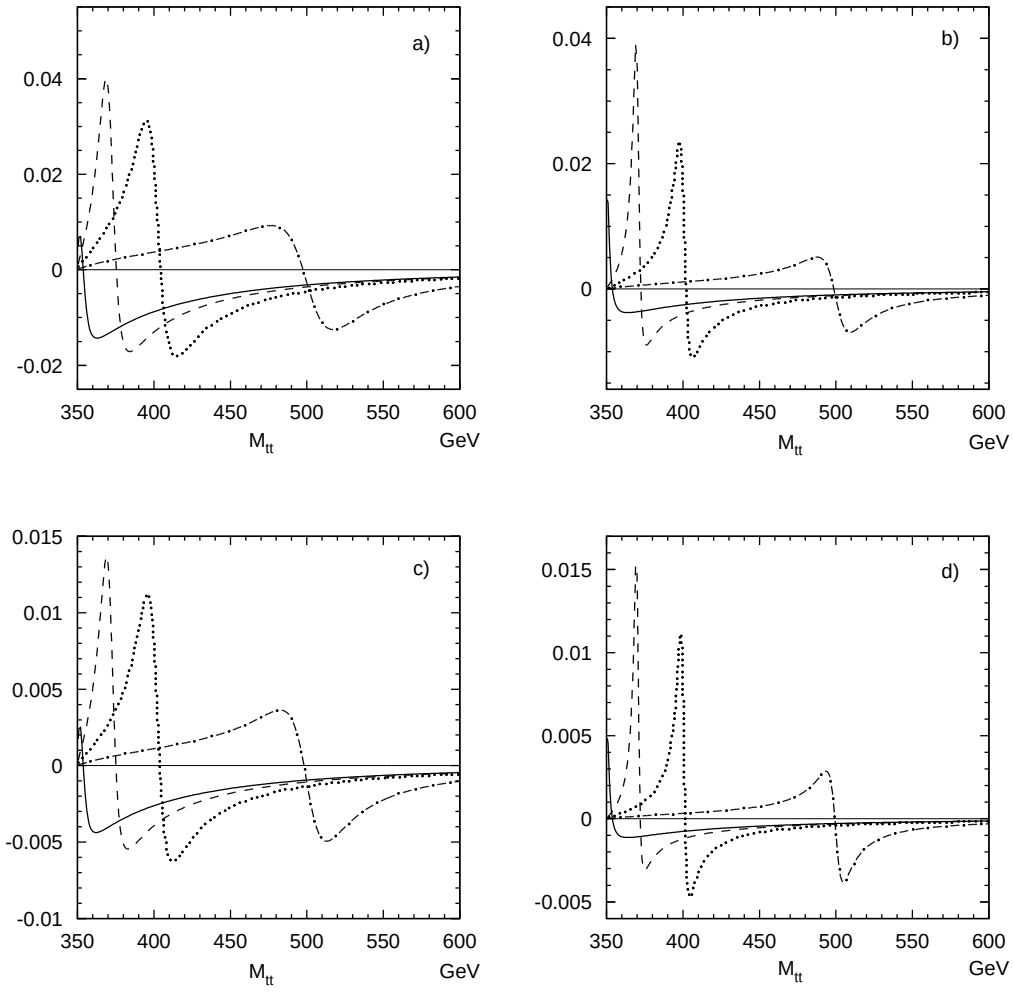
a)
b)
c)
d)
0.04
0.02
0
-0.02
0.015
0.01
0.005
-0.005
-0.01
350
400
450
500
550
600
M_{tt}
GeV

Figure 4

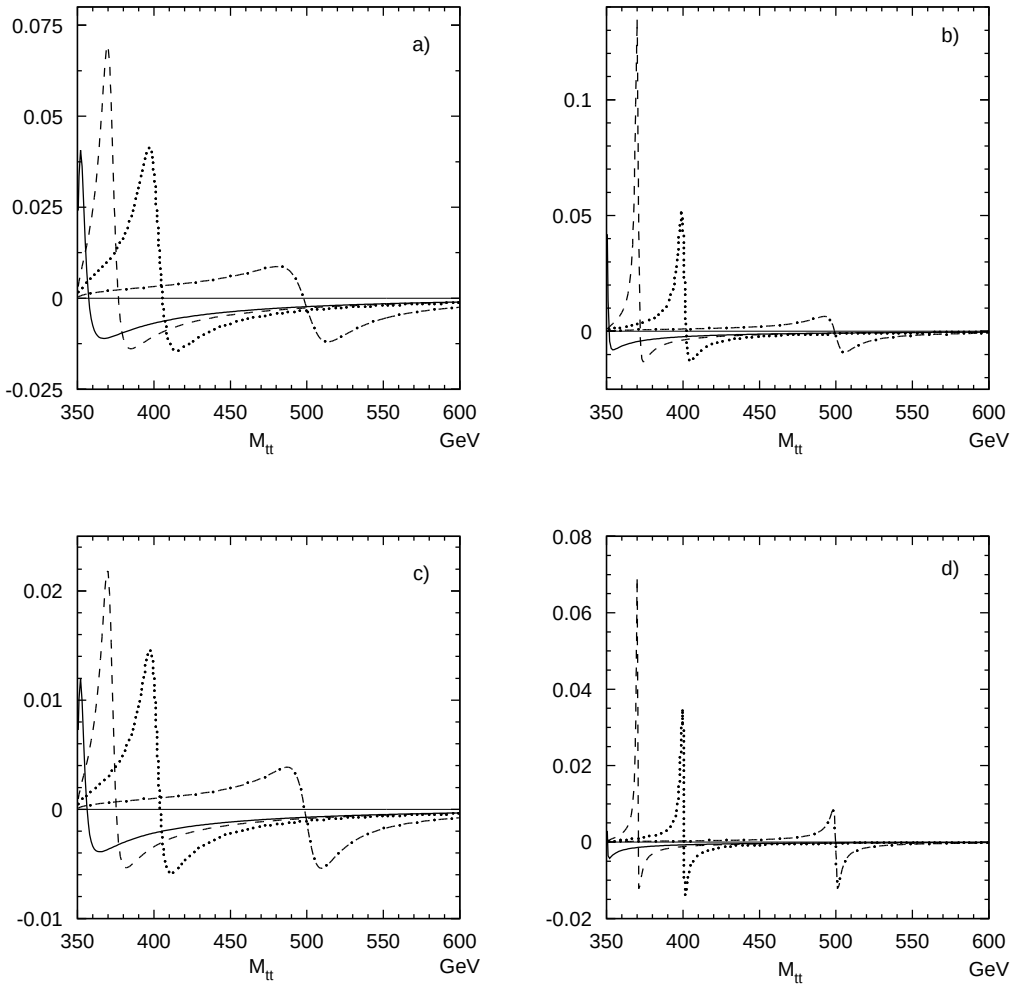
a)
b)
c)
d)
0.075
0.05
0.025
0
-0.025
0.1
0.05
0
0.02
0.01
0
-0.01
0.08
0.06
0.04
0.02
0
-0.02
350
400
450
500
550
600
M_{tt}
GeV

Figure 5

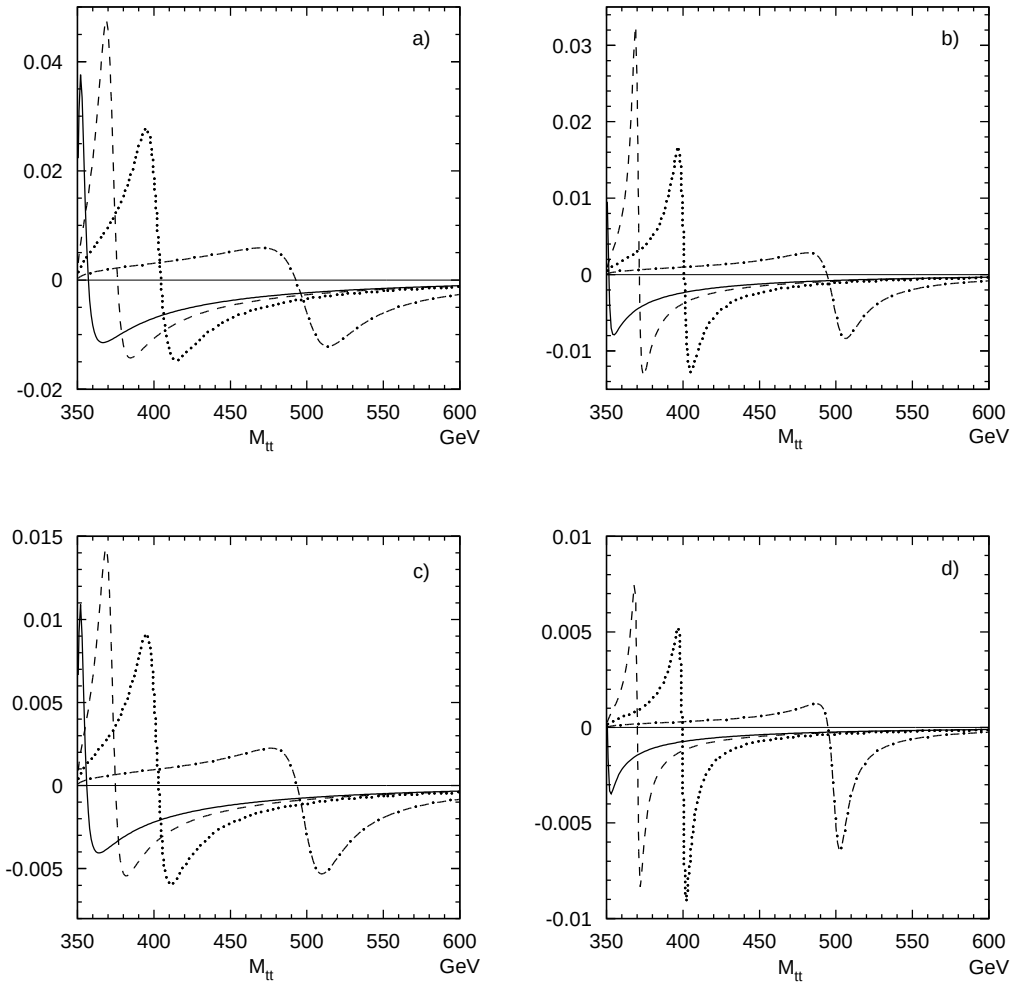
a)
b)
c)
d)
0.04
0.02
0
-0.02
0.03
0.01
-0.01
0.015
0.005
-0.005
350
400
450
500
550
600
M_{tt}
GeV

Figure 6

Tables

	below m_φ		above m_φ	
m_φ	$M_{t\bar{t}}$	$\Delta M_{t\bar{t}}$	$M_{t\bar{t}}$	$\Delta M_{t\bar{t}}$
320	–	–	$350-450$	100
350	–	–	$360-400$	40
370	$355-370$	15	$375-420$	45
400	$360-400$	40	$405-450$	45
500	$420-500$	80	$500-560$	60

Table 1

	g_{VV}					
m_φ	0.0		0.2		0.4	
370	2.7	9.4	2.7	9.3	2.6	8.6
	1.9	5.9	1.9	5.7	1.6	4.6
	0.86	3.0	0.87	3.0	0.83	2.7
	0.73	2.2	0.65	1.9	0.53	1.5
400	1.9	11.1	1.9	10.8	1.8	10.1
	1.0	5.7	0.95	5.3	0.83	4.5
	0.63	3.6	0.62	3.5	0.58	3.3
	0.41	2.3	0.36	2.0	0.29	1.6
500	0.69	5.4	0.67	5.3	0.61	4.8
	0.31	2.4	0.29	2.3	0.26	2.0
	0.25	1.9	0.24	1.9	0.21	1.7
	0.14	1.1	0.12	0.97	0.10	0.76

Table 2

m_φ	g_{VV} 0.0		0.2		0.4	
320	−0.63	5.3	−0.63	5.3	−0.62	5.3
	−0.18	1.6	−0.18	1.6	−0.18	1.6
	−0.19	1.6	−0.19	1.6	−0.19	1.6
	−0.06	0.47	−0.06	0.47	−0.05	0.47
350	−1.3	6.7	−1.3	6.6	−1.2	6.3
	−0.36	1.9	−0.36	1.9	−0.34	1.8
	−0.38	2.0	−0.38	2.0	−0.37	1.9
	−0.11	0.57	−0.11	0.57	−0.10	0.55
370	−1.4	8.1	−1.3	7.8	−1.2	7.1
	−0.51	3.1	−0.50	3.0	−0.46	2.8
	−0.43	2.5	−0.41	2.4	−0.38	2.2
	−0.16	0.95	−0.15	0.92	−0.14	0.85
400	−1.4	8.6	−1.4	8.3	−1.3	7.5
	−0.60	3.6	−0.58	3.5	−0.53	3.2
	−0.47	2.8	−0.45	2.7	−0.41	2.5
	−0.19	1.2	−0.18	1.1	−0.17	1.0
500	−0.96	5.4	−0.93	5.2	−0.83	4.6
	−0.46	2.6	−0.43	2.4	−0.36	2.0
	−0.36	2.0	−0.34	1.9	−0.30	1.7
	−0.23	1.3	−0.19	1.1	−0.15	0.82

Table 3

m_φ	g_{VV} 0.0		0.2		0.4	
370	4.4	29.8	4.1	27.4	3.3	20.9
	3.9	23.4	2.9	16.7	1.6	9.0
	1.3	8.7	1.2	8.0	0.98	6.1
	1.2	6.6	0.75	4.1	0.39	2.1
400	2.3	24.4	2.1	22.8	1.8	18.7
	1.3	13.4	1.1	11.1	0.75	7.5
	0.73	7.8	0.67	7.1	0.55	5.8
	0.49	4.9	0.35	3.5	0.21	2.1
500	0.65	8.6	0.59	7.9	0.46	6.0
	0.31	4.1	0.26	3.5	0.18	2.4
	0.24	3.2	0.22	2.9	0.16	2.1
	0.14	1.9	0.10	1.4	0.06	0.77

Table 4

m_φ	g_{VV} 0.0		0.2		0.4	
320	−0.61	9.2	−0.61	9.2	−0.61	9.2
	−0.19	3.0	−0.19	3.0	−0.19	3.0
	−0.19	2.8	−0.19	2.8	−0.19	2.8
	−0.06	0.91	−0.06	0.91	−0.06	0.91
350	−1.1	10.0	−1.1	10.1	−1.1	10.2
	−0.40	4.0	−0.40	4.0	−0.41	4.0
	−0.34	3.3	−0.35	3.3	−0.35	3.3
	−0.13	1.3	−0.13	1.3	−0.13	1.3
370	−1.0	10.6	−1.0	10.7	−1.1	11.1
	−0.50	5.4	−0.51	5.5	−0.52	5.6
	−0.37	3.9	−0.37	3.9	−0.38	4.0
	−0.17	1.9	−0.17	1.9	−0.17	1.9
400	−1.1	11.3	−1.1	11.4	−1.2	11.9
	−0.55	5.8	−0.56	5.8	−0.57	6.0
	−0.41	4.2	−0.42	4.3	−0.42	4.3
	−0.19	2.0	−0.20	2.1	−0.20	2.1
500	−0.92	8.2	−0.94	8.4	−0.98	8.8
	−0.46	4.1	−0.48	4.3	−0.49	4.4
	−0.35	3.2	−0.36	3.3	−0.38	3.4
	−0.24	2.1	−0.25	2.2	−0.23	2.1

Table 5

m_φ	g_{VV} 0.0		0.2		0.4	
370	2.7	16.6	2.7	16.1	2.6	14.9
	1.8	9.8	1.9	9.6	1.6	7.8
	0.84	5.1	0.87	5.2	0.84	4.7
	0.76	3.9	0.66	3.3	0.53	2.6
400	1.9	19.0	1.9	18.4	1.8	17.2
	1.0	9.5	0.96	9.0	0.84	7.8
	0.64	6.2	0.62	6.1	0.59	5.6
	0.42	3.8	0.36	3.4	0.29	2.7
500	0.70	8.9	0.68	8.7	0.63	8.0
	0.31	4.0	0.30	3.8	0.26	3.3
	0.25	3.2	0.24	3.1	0.22	2.8
	0.14	1.8	0.13	1.6	0.10	1.3

Table 6

m_φ	g_{VV} 0.0		0.2		0.4	
320	−0.64	9.1	−0.64	9.0	−0.64	9.0
	−0.19	2.7	−0.19	2.7	−0.19	2.7
	−0.19	2.7	−0.19	2.7	−0.19	2.7
	−0.06	0.80	−0.06	0.80	−0.06	0.80
350	−1.3	11.3	−1.3	11.2	−1.2	10.8
	−0.36	3.3	−0.36	3.2	−0.35	3.1
	−0.40	3.4	−0.39	3.4	−0.37	3.2
	−0.11	1.0	−0.11	1.0	−0.10	0.9
370	−1.4	13.5	−1.3	13.1	−1.2	11.9
	−0.52	5.2	−0.51	5.1	−0.47	4.7
	−0.44	4.2	−0.42	4.1	−0.38	3.7
	−0.16	1.6	−0.15	1.6	−0.14	1.4
400	−1.5	14.3	−1.4	13.7	−1.3	12.5
	−0.61	6.0	−0.59	5.9	−0.54	5.4
	−0.48	4.7	−0.46	4.5	−0.42	4.1
	−0.19	1.9	−0.19	1.9	−0.17	1.7
500	−0.99	8.7	−0.95	8.3	−0.85	7.4
	−0.47	4.2	−0.44	3.9	−0.37	3.3
	−0.37	3.2	−0.35	3.1	−0.30	2.7
	−0.23	2.1	−0.20	1.8	−0.15	1.3

Table 7

m_φ	g_{VV} 0.0		0.2		0.4	
370	3.5	26.4	3.3	24.3	2.7	18.7
	3.1	20.4	2.4	14.8	1.3	7.9
	1.1	7.7	0.98	7.0	0.80	5.5
	0.93	5.8	0.61	3.7	0.32	1.9
400	1.8	21.4	1.7	20.2	1.4	16.6
	1.0	11.8	0.88	9.9	0.60	6.7
	0.59	6.9	0.55	6.3	0.45	5.1
	0.39	4.3	0.28	3.1	0.17	1.9
500	0.52	7.6	0.47	7.0	0.37	5.3
	0.24	3.6	0.21	3.1	0.14	2.1
	0.19	2.8	0.17	2.5	0.13	1.9
	0.12	1.7	0.08	1.2	0.05	0.68

Table 8

m_φ	g_{VV} 0.0		0.2		0.4	
320	−0.48	8.1	−0.48	8.1	−0.48	8.1
	−0.15	2.6	−0.15	2.6	−0.15	2.6
	−0.15	2.5	−0.15	2.5	−0.15	2.5
	−0.05	0.80	−0.05	0.80	−0.05	0.80
350	−0.84	8.9	−0.85	8.9	−0.86	9.0
	−0.32	3.5	−0.32	3.5	−0.33	3.5
	−0.28	2.9	−0.28	2.9	−0.28	3.0
	−0.10	1.1	−0.10	1.1	−0.10	1.1
370	−0.81	9.4	−0.82	9.5	−0.86	9.9
	−0.41	4.8	−0.41	4.9	−0.42	4.9
	−0.30	3.4	−0.30	3.5	−0.31	3.5
	−0.14	1.6	−0.14	1.7	−0.14	1.7
400	−0.88	9.9	−0.89	10.1	−0.93	10.5
	−0.44	5.1	−0.45	5.2	−0.46	5.3
	−0.33	3.7	−0.33	3.8	−0.34	3.8
	−0.16	1.8	−0.16	1.8	−0.16	1.9
500	−0.73	7.2	−0.75	7.4	−0.78	7.8
	−0.37	3.7	−0.38	3.8	−0.39	3.9
	−0.28	2.8	−0.29	2.9	−0.30	3.0
	−0.19	1.9	−0.20	2.0	−0.18	1.8

Table 9